CMS

CERN-EP-2018-258
2019/03/28

CMS-B2G-17-014

arXiv:1810.03188v2 [hep-ex] 27 Mar 2019

Search for top quark partners with charge 5/3 in the same-sign dilepton and single-lepton final states in proton-proton collisions at $\sqrt{s} = 13\,\text{TeV}$

The CMS Collaboration[*]

Abstract

A search for the pair production of heavy fermionic partners of the top quark with charge 5/3 ($X_{5/3}$) is performed in proton-proton collisions at a center-of-mass energy of 13 TeV with the CMS detector at the CERN LHC. The data sample analyzed corresponds to an integrated luminosity of $35.9\,\text{fb}^{-1}$. The $X_{5/3}$ quark is assumed always to decay into a top quark and a W boson. Both the right-handed and left-handed $X_{5/3}$ couplings to the W boson are considered. Final states with either a pair of same-sign leptons or a single lepton are studied. No significant excess of events is observed above the expected standard model background. Lower limits at 95% confidence level on the $X_{5/3}$ quark mass are set at 1.33 and 1.30 TeV respectively for the case of right-handed and left-handed couplings to W bosons in a combination of the same-sign dilepton and single-lepton final states.

[*]See Appendix A for the list of collaboration members

1 Introduction

The prediction of new heavy quarks is a common feature of many theories of physics beyond the standard model (SM). In composite Higgs models [1–3], heavy partners of the SM top quark solve the hierarchy problem caused by quadratic divergences in the quantum-loop corrections to the Higgs boson mass by providing contributions that offset those due to the SM top quark. Often in such models, new color-triplet partners are predicted, with one of them having an exotic electric charge of 5/3 times the charge of the positron, referred to as $X_{5/3}$. In partially composite scenarios [4], these exotically charged fermions need not contribute to the gluon-gluon fusion production mode of the Higgs boson [5] and hence such measurements set no constraints on the mass of the $X_{5/3}$ particle. This paper describes a search for such a fermionic top quark partner, using proton-proton (pp) collision data collected during 2016 at a center-of-mass energy of 13 TeV with the CMS experiment at the CERN LHC, corresponding to an integrated luminosity of 35.9 fb^{-1}.

The dominant mechanism for $X_{5/3}$ production, shown in Fig. 1, is via quantum chromodynamics (QCD) processes, which yield particle-antiparticle pairs, since the $X_{5/3}$ carries color charge. The $X_{5/3}$ particle can also be singly produced via electroweak processes, but that production mode is model dependent and is not considered here. Since the pair production involves exclusively the SM QCD coupling, the tree-level cross section is independent of the $X_{5/3}$ properties, other than its mass. The $X_{5/3}$ particle is assumed to decay into a top quark and a W boson with a branching fraction of 100%, since this is the dominant decay mode in many models [6]. The decay can occur through either right-handed (RH) or left-handed (LH) couplings to W bosons, and this search presents results for either fully RH or fully LH decays. Thus we have not restricted the interpretation of the results to the case of vector-like quarks, whose left-handed and right-handed chirality states have the same transformation properties under the weak isospin SU(2) gauge group, although limits obtained with this assumption would be very similar to those set for pure-LH or pure-RH couplings.
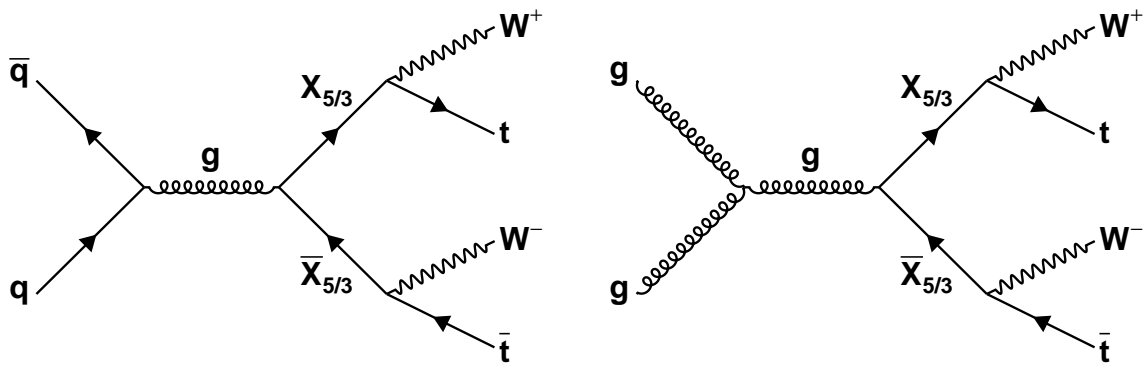

Figure 1: Leading order Feynman diagrams showing pair production and decays of $X_{5/3}$ particles via QCD processes.

This search focuses on two different final states consisting of either exactly one lepton or multiple leptons with the requirement that there be a pair of same-sign leptons. In both cases, additional hadronic activity in the event is required. Throughout the paper, the word lepton refers to an electron or a muon. Although leptonic tau decays are not specifically targeted in this analysis, their contribution to the signal efficiency is taken into account. The same-sign dilepton final state relies on its relatively clean signature and the large amount of jet activity from the other $X_{5/3}$ particle in the event to discriminate against background processes. The

single-lepton channel exploits the shape of the distribution of the visible mass of the top quark reconstructed in the detector to discriminate against background events.

Previously, CMS conducted a search for the $X_{5/3}$ particle using data collected at a center-of-mass energy of 8 TeV, corresponding to an integrated luminosity of 19.5 fb^{-1}, in the same-sign dilepton channel only, setting a lower limit on the $X_{5/3}$ mass of 800 GeV at 95% confidence level (CL) [7]. CMS has recently carried out another search [8] for $X_{5/3}$ in a combination of the same-sign dilepton and single-lepton final states using data collected in 2015 at $\sqrt{s} = 13$ TeV, corresponding to an integrated luminosity of 2.3 fb^{-1}, setting a lower limit on the $X_{5/3}$ mass of 1.02 (0.99) TeV for an RH (LH) coupling. Searches have also been performed by the ATLAS experiment at center-of-mass energies of 8 and 13 TeV [9–14]. The results based on $\sqrt{s} = 13$ TeV with 36.1 fb^{-1} of data set a lower limit of 1.37 TeV on the mass of the $X_{5/3}$ particle.

The present search follows closely the strategy of Ref. [8] and benefits from an order of magnitude increase in the integrated luminosity. This paper is organized as follows: Section 2 briefly describes the CMS detector; Section 3 discusses the simulated signal and background samples; in Section 4, trigger details are given; Section 5 contains a description of the event reconstruction; the analyses of the same-sign dilepton and single-lepton final states are detailed in Sections 6–7; and the systematic uncertainties are discussed in Section 8. Finally, Sections 9–10 give the results and a summary.

2 The CMS detector

The central feature of the CMS apparatus is a superconducting solenoid of 6 m internal diameter, providing a magnetic field of 3.8 T. Within the solenoid volume are a silicon pixel and strip tracker, a lead tungstate crystal electromagnetic calorimeter (ECAL), and a brass and scintillator hadron calorimeter (HCAL), each composed of a barrel and two endcap sections. Forward calorimeters extend the pseudorapidity (η) coverage provided by the barrel and endcap detectors. Muons are detected in gas-ionization chambers embedded in the steel flux-return yoke outside the solenoid. Events of interest are selected using a two-tiered trigger system [15]. The first level, composed of custom hardware processors, uses information from the calorimeters and muon detectors to select events at a rate of around 100 kHz within a time interval of less than 4 μs. The second level, known as the high-level trigger, consists of a farm of processors running a version of the full event reconstruction software optimized for fast processing, and reduces the event rate to less than 1 kHz before data storage.

A more detailed description of the CMS detector, together with a definition of the coordinate system used and the relevant kinematic variables, can be found in Ref. [16].

3 Simulation

The $X_{5/3}$ signal processes are generated using a combination of MADGRAPH5_aMC@NLO 2.2.2 [17] and MADSPIN [18] for two coupling scenarios: allowing only RH or only LH $X_{5/3}$ coupling to W bosons. The MADGRAPH5_aMC@NLO event generator is used both to produce $X_{5/3}$ events and to decay each $X_{5/3}$ to a top quark and a W boson, while the decays of the top quarks and W bosons are simulated with MADSPIN. The signal events are simulated at leading order (LO) for $X_{5/3}$ masses from 800 to 1500 GeV, in 100 GeV steps, separately for each coupling scenario. The signal samples are then normalized to the next-to-next-to-leading order cross sections using the TOP++2.0 generator [19–24], with resummation of soft gluon corrections at the next-to-next-to-leading logarithmic accuracy.

A variety of event generators are used for the Monte Carlo (MC) simulation of the background processes. The POWHEG 2.0 [25–28] event generator is used to simulate $t\bar{t}$, single top quark events in the t-channel and tW channel, $t\bar{t}$H, WZ, and ZZ events to next-to-leading order (NLO) precision. The MADGRAPH5_aMC@NLO event generator is used to simulate Z+jets, W+jets, single top quark process in the s-channel, $t\bar{t}$Z, $t\bar{t}$W, and $t\bar{t}t\bar{t}$ processes, events with a combination of three W or Z bosons, and QCD multijet events. The Z+jets, W+jets, WW, and QCD multijet processes are generated at LO using the MLM matching scheme [29]. The FxFx matching scheme [30] is used for $t\bar{t}$Z, $t\bar{t}$W, $t\bar{t}t\bar{t}$, triboson, and single top quark process in the s-channel, which are generated at NLO.

Additional pp interactions in the same or neighboring bunch crossings (pileup) are modeled by superimposing simulated minimum-bias interactions onto the simulated events for all processes. Simulated events are reweighted so that the number of pileup interactions matches the distribution observed in data.

Parton showering, hadronization, and the underlying event are simulated with PYTHIA 8.212 [31], using NNPDF 3.0 [32] parton distribution functions (PDFs) and the CUETP8M1 tune [33, 34] for all MC processes, except for the $t\bar{t}$ sample, which is produced with the CUETP8M2T4 tune [35]. Finally, for all MC samples, generated events are processed through the full GEANT4-based simulation of the CMS detector [36] and then reconstructed using the same procedure as the data.

The transverse momentum (p_T) spectrum of the top quarks in $t\bar{t}$ events is known to be mismodeled in simulation [37] and, therefore, corrections are applied to simulated $t\bar{t}$ events as a function of the top quark p_T.

Many of the SM background processes in this search are similar and are therefore grouped together in the discussion that follows. The same-sign dilepton final state groups SM processes according to their similarity to the signal topology and classifies them as "$t\bar{t}$+X", containing $t\bar{t}$W, $t\bar{t}$Z, $t\bar{t}$H, and $t\bar{t}t\bar{t}$, which are those processes most similar to the signal, and "multiboson", comprising all processes mentioned above where two or three electroweak bosons are directly produced. For the single-lepton final state, the background processes are grouped into three categories. The first category is referred to as "TOP", which is dominated by $t\bar{t}$ events, but also includes any process having at least one top quark. The second category is referred to as "EWK", which is dominated by W+jets events, but includes all processes that contain electroweak bosons and no top quark. The third category is referred to as "QCD" and is the QCD multijet background.

4 Trigger and event selection

For the same-sign dilepton final state, candidate events are required to have passed triggers based on two electrons, two muons, or electron-muon combinations. For the first half of the data set, symmetric trigger p_T thresholds were used for the dielectron and electron-muon triggers, corresponding to a p_T requirement of 33 (30) GeV for the former (latter). During the data-taking period, the instantaneous luminosity of the LHC steadily increased. Therefore, for the second half of the data set, to keep the trigger rate at an acceptable level, these triggers were replaced with new ones that had asymmetric p_T requirements, with the higher p_T (leading) lepton requirement of 37 GeV and the lower p_T (subleading) lepton threshold of 27 GeV, for both the dielectron and electron-muon triggers. Throughout the entire data taking period, the same dimuon trigger, which had p_T requirements of 30 (11) GeV for the leading (subleading) muon, was used.

In the single-lepton final state, events are required to pass either single-electron or single-muon triggers. For the single-electron triggers, either an electron isolated from nearby particles with $p_T > 32\,\text{GeV}$, or a very loosely isolated electron with $p_T > 15\,\text{GeV}$ together with $H_T > 350\,\text{GeV}$ is required, where H_T is the scalar p_T sum of all jets at the trigger level with $p_T > 30\,\text{GeV}$ and $|\eta| < 3.0$. The single-muon triggers require either a muon with $p_T > 50\,\text{GeV}$ with no isolation requirement or a very loosely isolated muon with $p_T > 15\,\text{GeV}$ together with $H_T > 350\,\text{GeV}$.

5 Object reconstruction

This search makes use of electrons, muons, jets, and missing transverse momentum. The reconstruction of these objects is based on a particle-flow (PF) algorithm [38], which reconstructs and identifies particles using an optimized combination of subdetector information.

The candidate events are required to have at least one reconstructed vertex passing basic quality criteria. In the case that there are multiple reconstructed vertices, the one with the largest value of summed physics-object p_T^2 is taken to be the primary pp interaction vertex. Here, the physics objects are the jets, clustered using the jet finding algorithm [39, 40] with the tracks assigned to the vertex as inputs, and the associated missing transverse momentum, taken as the negative vector p_T sum of those jets.

Electron candidates are reconstructed from a collection of electromagnetic clusters that are matched to reconstructed tracks in the tracker [41]. As in Ref. [8], the identification criteria for electrons are based on a multivariate analysis (MVA), which makes use of shower shape variables, track quality requirements, variables measuring compatibility between the track and matched electromagnetic clusters, distance from the track to the primary vertex, and the probability that the electron candidate arises from a photon conversion.

In the same-sign dilepton final state, a consistency requirement is placed on the three measurements of the electron charge that result from three different methods. Two of these charge assignment methods are based solely on tracker information, where the charge of the track is determined by the standard CMS track reconstruction [42] or the Gaussian Sum Filter algorithm [43]. A third method is based on the difference in azimuthal angle (ϕ) between the ECAL cluster center of gravity and pixel detector seeds used to reconstruct the electron track. Because the third method has been found to be unreliable at high p_T, only the results from the first two charge determination methods are required to agree for electrons with p_T above $100\,\text{GeV}$. Relaxing the requirement on this method recovers 5–10% of signal efficiency, depending on the mass of the $X_{5/3}$. For electrons with p_T below $100\,\text{GeV}$, all three charge measurements are required to agree.

Muons are reconstructed using a global track fit of hits in the muon chambers and hits in the silicon tracker. The identification criteria are based on the number of hits used in the fit, the track quality, and the distance of the track to the primary vertex. For the same-sign dilepton final state in the dimuon channel, the two muons should not be both within $|\eta| > 1.2$, unless they are in opposite sides of the detector in η or are well separated in ϕ ($\Delta\phi > 1.25\,\text{rad.}$). This last requirement is imposed because of a misconfiguration of part of the trigger system, in the first part of the data-taking period, affecting nearby muons in the endcap detectors and has no effect on signal efficiency.

We select charged leptons that are isolated from other activity in the detector. The isolation variable (I) for both electrons and muons is defined as the scalar p_T sum of all PF candidates within a cone of varying size around the particle, divided by its p_T. The radius used for the

isolation cone ($\mathcal{R}$) is defined as:

$$\mathcal{R} = \frac{10\,\text{GeV}}{\min(\max(p_{\text{T}}, 50\,\text{GeV}), 200\,\text{GeV})},$$ (1)

where the lepton p_{T} is measured in GeV. Corrections are applied to the computation of the lepton isolation in order to account for the effect of pileup using the effective area method [44]. Two categories of leptons are defined, a "tight" lepton, which has $I < 0.1$ and also passes the relevant identification criteria above, and a "loose" lepton, which has $I < 0.4$. In addition, the definition of "loose" electrons includes a relaxed requirement on the MVA discriminant, and "loose" muons have relaxed requirements on several of the aforementioned identification requirements. The signal efficiencies for "tight" and "loose" electrons (muons) are $\approx$88% ($\approx$97%) and $\approx$95% ($\approx$100%) for $|\eta| < 2.5$ (2.4), respectively, excluding the barrel-endcap transition region (1.44 $< |\eta| <$ 1.57) for electrons.

Data-to-simulation scale factors to correct for imperfect detector simulation are obtained using the "tag-and-probe" method [45] for lepton trigger, identification, and isolation, as functions of the lepton p_{T} and η.

Jets are clustered from the reconstructed PF candidates using the anti-k_{T} algorithm [39] implemented in the FASTJET package [40, 44, 46] with a distance parameter of 0.4 (AK4) and are required to satisfy $p_{\text{T}} > 30\,\text{GeV}$ and $|\eta| < 2.4$. Additional selection criteria are applied to remove spurious energy deposits originating from isolated noise patterns in certain HCAL regions and from anomalous signals caused by particles depositing energy in the silicon avalanche photodiodes used in the ECAL barrel region [47]. Jets that overlap with leptons have the four-momentum of any shared lepton subtracted from the jet four-momentum. Jet energy corrections are applied for residual nonuniformity, nonlinearity of the detector response, and the level of pileup in the event [48, 49].

In the single-lepton final state analysis, jets are tagged as originating from the decay of a bottom quark using a combined secondary vertex (CSVv2) algorithm [50], which classifies jets based on the distance between their vertex and the primary vertex, along with observables such as track impact parameter. At the working point chosen, the efficiency for correctly tagging jets from bottom quark decays is between 40–65%, depending on the jet p_{T}. The efficiency of tagging charm hadron jets is approximately 12%, averaged over jet p_{T}, while the probability of mistagging light-flavor jets is roughly 1%.

Large-radius jets are also reconstructed using the anti-k_{T} algorithm, with a distance parameter of 0.8 (AK8), and are used to tag hadronic decays of Lorentz-boosted top quarks or W bosons in the single-lepton final state analysis. Two variables are used to classify AK8 jets as originating from merged top quark decays (t tagging): the jet mass after grooming with the soft-drop algorithm [51] and the ratio of N-subjettiness variables τ_3/τ_2 [52], a variable that provides strong discrimination between AK8 jets with two and three subjets. For an AK8 jet to be labeled as t tagged, it must have $p_{\text{T}} > 400\,\text{GeV}$, soft-drop mass between 105 and 220 GeV, and the ratio τ_3/τ_2 less than 0.81. This set of t tagging requirements yields an efficiency of roughly 60% and a mistag rate of roughly 3% for the p_{T} range considered. Data-to-simulation scale factors [47] are applied to events containing t-tagged jets in order to match the performance in the simulation to that seen in data.

If an AK8 jet fails the top quark identification criteria, it is considered for classification as a merged hadronic W boson decay (W tagging). An AK8 jet is labeled as W tagged if it has $p_{\text{T}} > 200\,\text{GeV}$, pruned mass between 65 and 105 GeV, and a ratio of N-subjettiness variables τ_2/τ_1 smaller than 0.6, where the pruned mass is the mass of the jet after removing the soft

and wide-angle radiated partons [53]. This set of requirements used to select W-tagged jets yields a signal efficiency of 60–80% and a mistag rate of 20–5%, depending on the p_T of the AK8 jet. The pruned mass scale is found to be consistent between data and simulation, but the mass resolution is found to be better in simulation and hence it is smeared in simulated events to match the resolution seen in data. Data-to-simulation scale factors [47] are also applied in order to match the performance of the W tagging in simulation to that seen in data.

The missing transverse momentum ($\vec{p}_T^{\,\text{miss}}$) is defined as the negative of the vector p_T sum of all reconstructed PF candidates in an event and its magnitude is denoted as p_T^{miss}. Energy scale corrections applied to jets are also propagated to p_T^{miss}.

6 Same-sign dilepton final state

The search in the same-sign dilepton final state takes advantage of the rare signature of same-sign leptons, as well as the significant number of other high-p_T leptons and jets from the decay of the other $X_{5/3}$ particle in the event.

The background contributions associated with this channel fall into three main categories: same-sign prompt leptons (SSP), opposite-sign prompt leptons (ChargeMisID), and same-sign nonprompt dilepton (Nonprompt). The SSP background consists of SM processes that give prompt, same-sign dilepton signatures, where a prompt lepton is defined as one originating from the direct decay of either a W or Z boson. The contribution of these processes to the signal region is estimated using simulation. The ChargeMisID background is composed of events that contain two opposite-sign leptons, but have the charge of one lepton mismeasured. This contribution is estimated from data. The Nonprompt background consists of events that contain at least one nonprompt lepton passing the lepton selection criteria. Such events arise from jets misidentified as leptons, nonprompt leptons from heavy-flavor decays or conversions in the detector material, etc. This contribution is also estimated using control samples in data.

We first require two same-sign leptons that pass the tight definition given in Section 5. The same-sign lepton pair that maximizes the scalar p_T sum of its constituents is taken as the signal pair. Because the same-sign dilepton final state sample was collected in two different triggering eras, different p_T requirements are placed on the pair according to the triggering era in order to ensure that the trigger has reached full efficiency. For the early (late) triggering era, the leading lepton is required to have $p_T > 40\,(40)\,\text{GeV}$ while the subleading lepton is required to have $p_T > 35\,(30)\,\text{GeV}$.

A set of preselection requirements is defined as follows. First, the invariant mass of the same-sign lepton pair is required to be greater than 20 GeV (quarkonia veto) and the event is required to contain at least two AK4 jets passing the requirements outlined above. Second, events containing a Z boson are removed by vetoing any event with an opposite-sign, same-flavor pair of leptons having an invariant mass within 15 GeV of the mass of the Z boson. For the dielectron channel, this requirement is extended to the pair of same-sign electrons as well, in order to veto ChargeMisID background events. This eliminates the majority of Drell–Yan (DY) events, which would otherwise be a major contributor to the ChargeMisID background, without adversely affecting our signal efficiency.

After the preselection, two analysis-specific variables are defined as follows. The number of constituents (N_{const}) is the number of AK4 jets in the event together with the number of additional (i.e. not in the same-sign pair) leptons passing the tight definition. The H_T^{lep} variable is the scalar p_T sum of all constituents including the same-sign pair.

The criteria on these two variables are optimized for expected signal significance and the final requirements are $N_{\text{const}} \geq 5$ and $H_{\text{T}}^{\text{lep}} > 1200\,\text{GeV}$. Figure 2 shows the $H_{\text{T}}^{\text{lep}}$ distributions at the preselection level; the distributions of the N_{const} variable (not shown) were also confirmed to be well described.

6.1 Background modeling

In this section, we summarize the background modeling used in the same-sign dilepton search. The estimated contribution for all backgrounds is presented in Table 1. For additional details see Ref. [8].

6.1.1 Same-sign prompt lepton background

The SSP background consists of processes with multiple W or Z bosons decaying to leptons, the bosons themselves either being created directly or through the decay of a top quark. The contributions from these processes are estimated using the simulation as described in Section 3. The systematic uncertainties included for the SSP background are discussed in Section 8.

6.1.2 Opposite-sign prompt lepton background

Background events in the ChargeMisID category arise from a pair of opposite-sign prompt leptons where the charge of one lepton is mismeasured, yielding a pair of same-sign leptons. The charge misidentification probability for muons is much smaller and hence is considered negligible [54]. For electrons, the probability of charge misidentification is measured using observed DY events by requiring a pair of electrons with an invariant mass (driven by ECAL information) between 81 and 111 GeV. The charge misidentification probability is binned by $|\eta|$ of the electron, and split into three different p_{T} regions: below 100 GeV, between 100 and 200 GeV, and above 200 GeV. These regions capture the effects of the differences in charge consistency requirements for low- and high-p_{T} electrons, as well as any remaining inherent dependence of the charge misidentification probability on the electron p_{T}. Values of the charge misidentification probability range from 10^{-4} for low-p_{T} electrons in the central part of the detector to a few percent for high-p_{T} electrons in the forward region of the detector.

To estimate the contribution of the ChargeMisID background, opposite-sign dilepton events that satisfy all signal region kinematic requirements are weighted by the relevant probability of charge misidentification according to the kinematics of the electron(s) in the opposite-sign pair.

To account for the differences seen in the overall charge misidentification rate between DY and $t\bar{t}$ events in simulation (roughly 25% higher in DY), and some small residual kinematic disagreements (p_{T} dependent variation of roughly 5% or less), a 30% systematic uncertainty is assigned to the estimate of the number of ChargeMisID background events.

6.1.3 Same-sign nonprompt background

The Nonprompt background arises from events where a nonprompt lepton (such as a lepton from a heavy-flavor decay, photon conversion, or a misidentified jet) passes the tight lepton identification requirements. Contributions from these types of events are estimated using the "Tight-Loose" method as described in Ref. [55]. This method relies on collecting a sample of dilepton events where the leptons are allowed to pass the loose definition described previously, and then scaling those events by weights involving the probability of a loose prompt lepton to pass the tight definition ("prompt rate") and the probability of a loose nonprompt lepton to pass the tight definition ("misidentification rate").
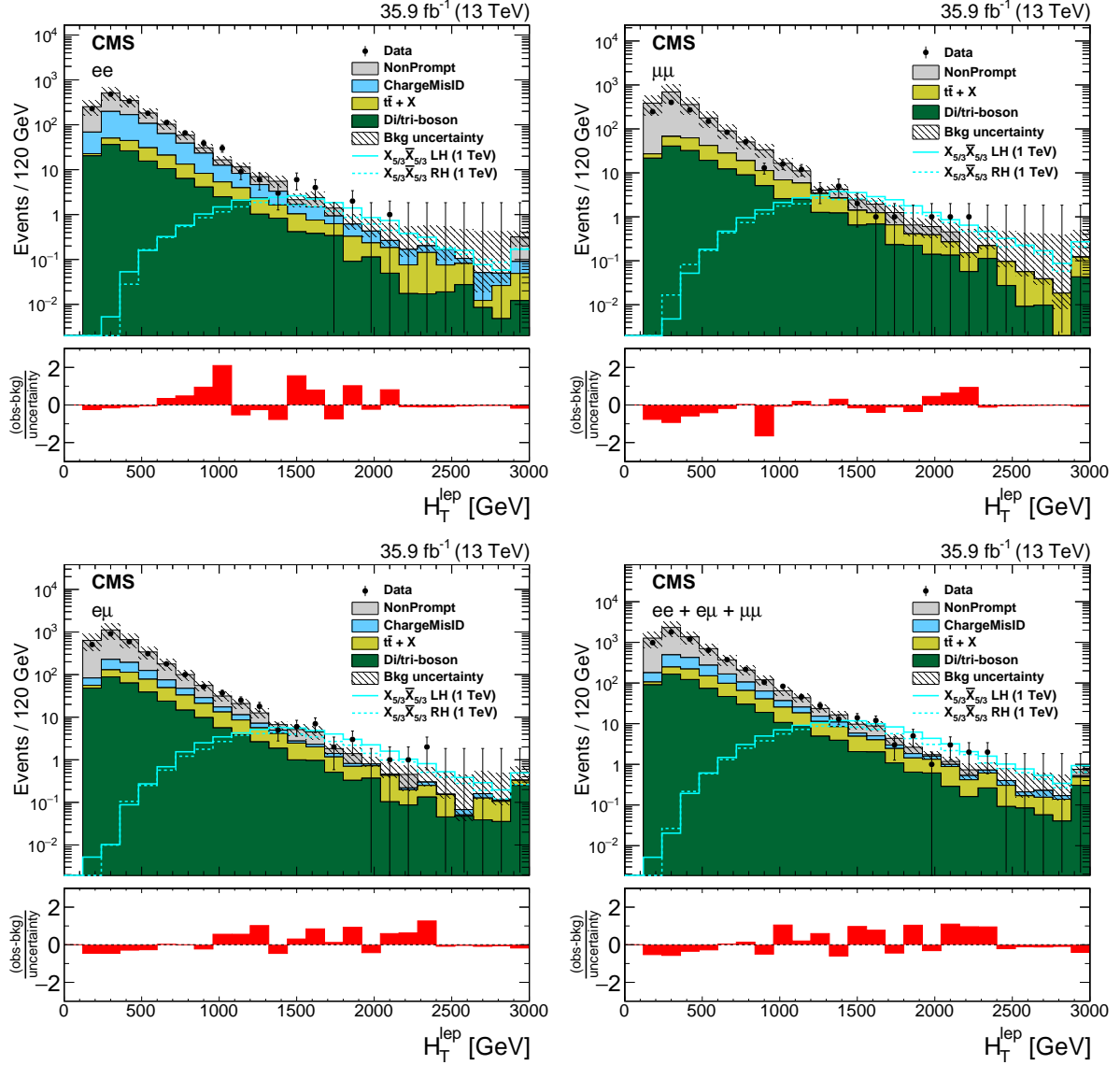
Figure 2: The H_T^{lep} distributions after the same-sign dilepton requirement, Z boson and quarkonia lepton invariant mass vetoes, and the requirement of at least two AK4 jets in the event, for dielectron (upper left), dimuon (upper right), electron-muon (lower left) final states, and their combination (lower right). The hatched area shows the combined systematic and statistical uncertainty in the background prediction for each bin. The last bin includes overflow events. The lower panel in each plot shows the difference between the observed and the predicted numbers of events divided by the total uncertainty. The total uncertainty is calculated as the sum in quadrature of the statistical uncertainty in the observed measurement and the uncertainty in the background, including both statistical and systematic components. Also shown are the expected signal distributions for a 1 TeV $X_{5/3}$ with LH (solid line) and RH (dashed line) couplings.

The prompt rate is determined using the "tag-and-probe" technique with DY-enriched dilepton data where the invariant mass of the leptons is within $10\,\mathrm{GeV}$ of the Z boson mass. For muons, the prompt rate is found to be flat to within a few percent as functions of η and p_T and hence the average of 0.94 is taken. The prompt rate for electrons is found to be flat versus η, but has a p_T dependence, which is taken into account and gives values for the prompt rate ranging from 0.80 to 0.95.

The misidentification rate is determined using a sample enriched in QCD multijet events. The selection of this sample follows the approach described in Ref. [8] and requires exactly one loose lepton, at least one jet, low p_T^{miss}, and low M_T, where M_T is the transverse mass of the lepton and p_T^{miss}. We also reject events if the invariant mass of the lepton and any jet is within $10\,\mathrm{GeV}$ of the Z boson mass.

Because of the significantly larger integrated luminosity used in this analysis, binning of the variation in the misidentification rate as a function of lepton η is possible; the values obtained range from 0.16 to 0.25 (0.34) for electrons (muons), with the lower values corresponding to leptons in the central part of the detector.

The uncertainty in the estimation of the Nonprompt background is derived by comparing the variation between the misidentification rates measured from different types of nonprompt lepton candidates, categorized by the generator-level origin of the nonprompt lepton; the variation in kinematic dependence of these misidentification rates with respect to p_T and η; and the overall level of closure seen in the method. The above checks are all performed using t$\bar{\mathrm{t}}$ MC events. To ensure that all effects are covered, a 50% uncertainty is assigned to the estimate of the Nonprompt background.

6.2   Event yields

Summing over the three dilepton final states, between 1.8 (2.4) and 3.4 (4.1)% of the produced $X_{5/3}$ pairs are expected to pass the full selection criteria for an LH (RH) signal, depending on the $X_{5/3}$ mass. The number of observed events, along with the expected number of background events broken down by category, is shown in Table 1. The background predictions in the table are derived after a "background-only" fit to the data as described in Section 9, where the signal strength is assumed to be zero. The fit increases the predicted Nonprompt background by less than its originally assigned uncertainty, and reduces the uncertainty associated with this background by about 30%. Also shown is the number of expected signal events for an RH $X_{5/3}$ with mass $1\,\mathrm{TeV}$. The observed number of events in the signal region categories are compatible with the background predictions.

Table 1: Summary of yields from simulated prompt same-sign dilepton (SSP MC), same-sign nonprompt (Nonprompt), and opposite-sign prompt (ChargeMisID) backgrounds after the full analysis selection. Also shown are the number of expected events for an RH $X_{5/3}$ particle with a mass of $1\,\mathrm{TeV}$. The uncertainties include both statistical and all systematic components (as described in Section 8). The number of events and uncertainties correspond to the background-only fit to data for the background, while for the signal they are based on the yields before the fit to data.

Channel	RH $X_{5/3}$ (1 TeV)	SSP MC	Nonprompt	ChargeMisID	Total bkg.	Data
Dielectron	11.6 ± 0.8	3.9 ± 0.3	4.6 ± 1.7	2.4 ± 0.7	10.9 ± 1.9	10
Dimuon	16.1 ± 1.2	5.7 ± 0.5	5.5 ± 1.9	—	11.2 ± 2.0	12
Electron-muon	26.9 ± 1.9	10.3 ± 0.8	11.3 ± 3.6	1.7 ± 0.5	23.2 ± 3.7	26

7 Single-lepton final state

The single-lepton final state targets events where one of the four W bosons in the event decays leptonically and the others decay hadronically (including hadronic tau decays). Events are required to have exactly one tight lepton with $p_T > 80\,\text{GeV}$. An event is discarded if it contains another lepton that passes the loose identification criteria and has $p_T > 10\,\text{GeV}$. In order to limit the background contributions from QCD multijet events, selected events are required to have $p_T^{\text{miss}} > 100\,\text{GeV}$ and the AK4 jet that is closest to the lepton is either required to be separated by $\Delta R > 0.4$, where $\Delta R = \sqrt{(\Delta \eta)^2 + (\Delta \phi)^2}$, or the magnitude of the lepton momentum that is transverse to the jet axis is required to be greater than $40\,\text{GeV}$.

Since the signal topology includes significant levels of hadronic activity, events are also required to have at least four AK4 jets, and the leading and subleading jets are required to have a p_T greater than 450 and $150\,\text{GeV}$, respectively. At least one of the four AK4 jets is required to pass the b tagging requirement.

Two observables are found to provide strong discrimination between signal and background events as in Ref. [8]: $\Delta R(\ell, j_2)$, the angular separation between the lepton and subleading AK4 jet, and $\min[M(\ell, b)]$, the minimum mass reconstructed using the lepton and any AK4 jet in the event passing the b tagging requirement. Signal regions for this search are constructed from events with $\Delta R(\ell, j_2) > 1.0$, with the distribution of $\min[M(\ell, b)]$ used for signal extraction. Figure 3 shows the distributions for $\Delta R(\ell, j_2)$ and $\min[M(\ell, b)]$ in events with at least three AK4 jets, including a leading (subleading) jet with $p_T > 250\,(150)\,\text{GeV}$ prior to the fit to data. The distribution of $\min[M(\ell, b)]$ for the background, dominated by $t\bar{t}$ events, features a sharp drop around $150\,\text{GeV}$, since, for such events, this variable represents the visible mass of the top quark in the detector. The $\Delta R(\ell, j_2)$ variable shows that the subleading jets populate both the same and opposite hemisphere relative to the lepton in the background events, whereas in the $X_{5/3}$ signal events, the subleading jet is usually opposite to the lepton.

7.1 Background modeling

All of the background processes in the single-lepton analysis are modeled using the simulation. In order to confirm that this modeling is correct, the agreement between simulation and data is checked for the dominant ($t\bar{t}$) and subdominant (W+jets) background processes using background-enriched control regions. The control regions have the same conditions as the signal region, with the requirement on $\Delta R(\ell, j_2)$ inverted such that $0.4 < \Delta R(\ell, j_2) < 1.0$. The W+jets enriched control region also requires that no jet passes the b tagging requirements, and is split into categories of either zero or at least one W-tagged jet. The $t\bar{t}$ enriched control region uses the b tagging requirements of the signal region and is split into either 1 or ≥ 2 b-tagged jet categories. With the lack of b-tagged jets in the W+jets control region, the reconstructed mass of interest is modified to be the minimum mass of the lepton and any AK4 jet in the event ($\min[M(\ell, j)]$).

The agreement between the data and the SM prediction from simulation is checked in all control region categories and is found to be within the uncertainties in the prediction, which are detailed in Section 8. Figure 4 shows the distributions of $\min[M(\ell, b)]$ and $\min[M(\ell, j)]$ for the $t\bar{t}$ and W+jets enriched control regions, while Table 2 shows the predicted and observed numbers of events in each control region after the full analysis selection. The background predictions in Fig. 4 and Table 2 are given after the background-only fit to data using all categories in both final states, including both signal and control regions.
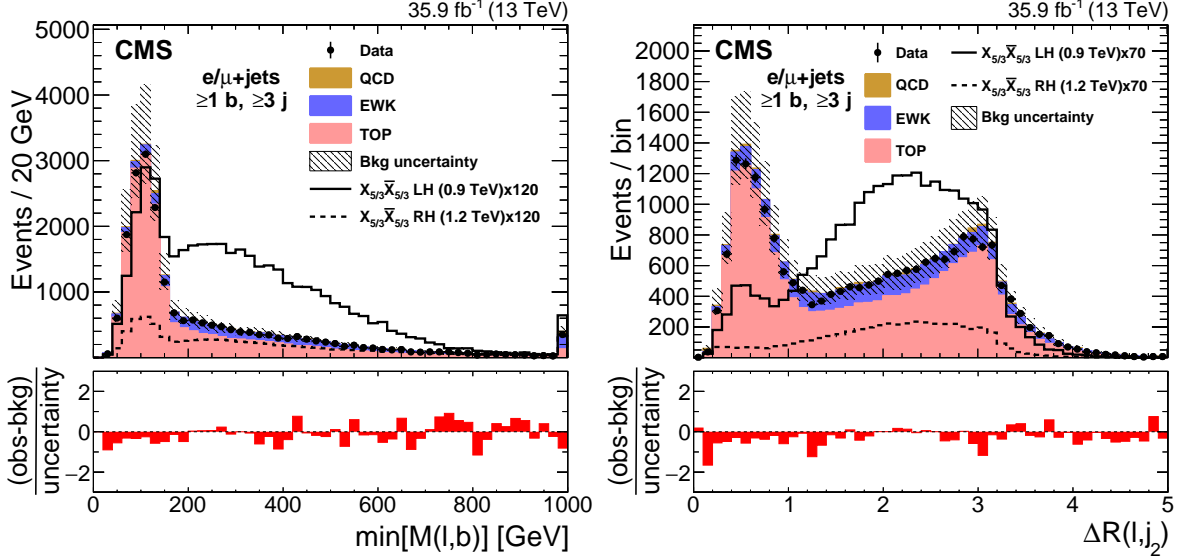
Figure 3: Distributions of $\min[M(\ell, b)]$ (left) and $\Delta R(\ell, j_2)$ (right) in data and simulation for events with at least three AK4 jets, including a leading (subleading) jet with $p_T > 250\,(150)\,\text{GeV}$, after combining the electron and muon channels. Example signal distributions are also shown, scaled by a factor of 120 (70) in the $\min[M(\ell, b)]$ ($\Delta R(\ell, j_2)$) distribution. The last bin includes overflow events. The lower panel in each plot shows the difference between the observed and the predicted numbers of events in that bin divided by the total uncertainty. The total uncertainty is calculated as the sum in quadrature of the statistical uncertainty in the observed measurement and the statistical and systematic uncertainties in the background.

Table 2: Expected (observed) numbers of background (data) events passing the final selection requirements, in the $t\bar{t}$ and W+jets control region ($0.4 < \Delta R(\ell, j_2) < 1.0$) categories, after combining the single-electron and single-muon channels. The numbers of events expected from two example signals are also shown. The event yields and their uncertainties correspond to the background-only fit to data for the background, while for the signal they are based on the values before the fit to data.

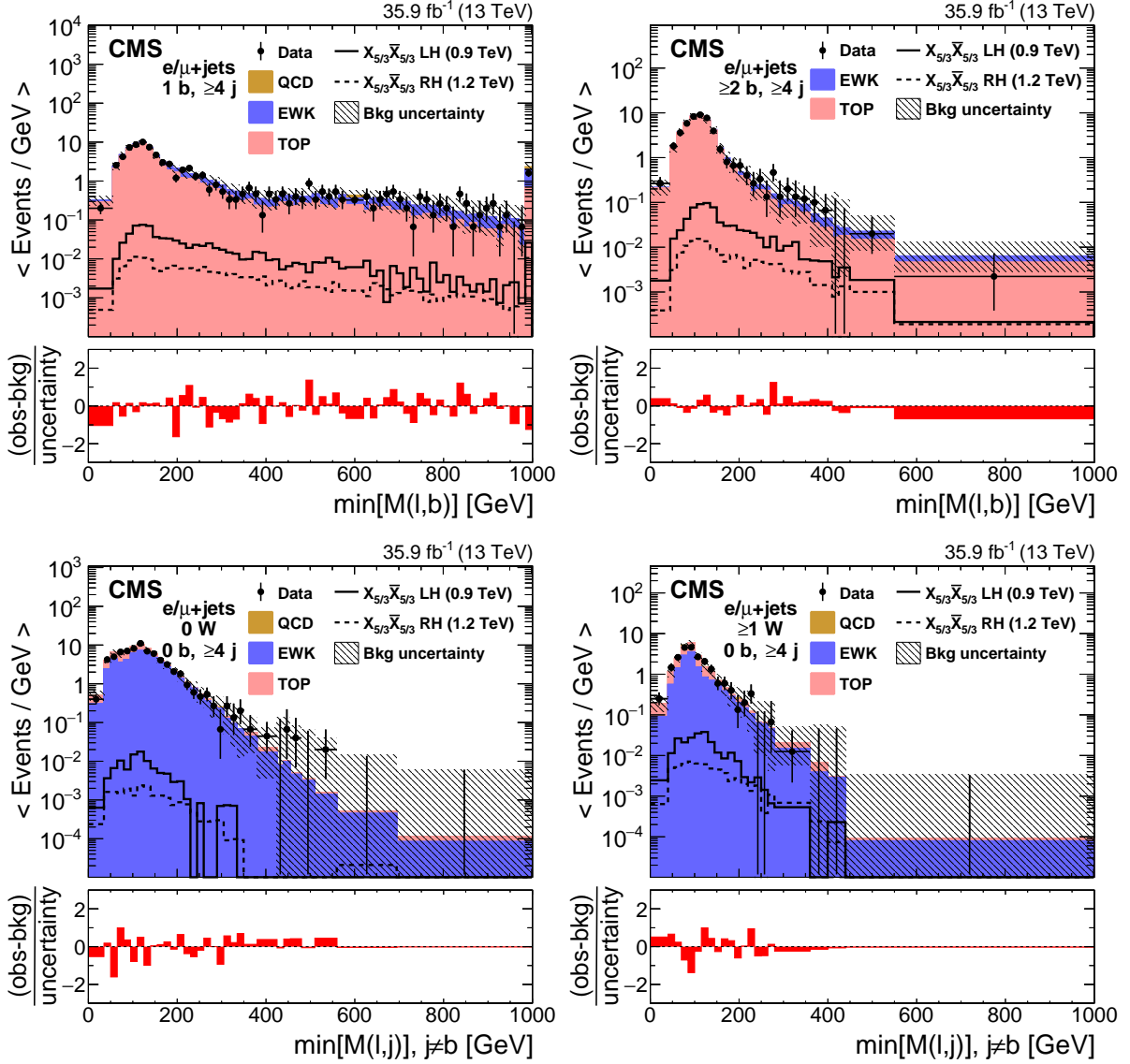| Sample	$\geq 0\,t, \geq 0\,W, 1\,b$	$\geq 0\,t, \geq 0\,W, \geq 2\,b$	$\geq 0\,t, 0\,W, 0\,b$	$\geq 0\,t, \geq 1\,W, 0\,b$
LH $X_{5/3}$ (0.9 TeV)	13.15 ± 0.61	10.90 ± 0.58	1.46 ± 0.27	3.60 ± 0.36
RH $X_{5/3}$ (1.2 TeV)	3.02 ± 0.13	2.34 ± 0.12	0.32 ± 0.06	1.00 ± 0.08
TOP	953 ± 97	668 ± 72	274 ± 30	134 ± 14
EWK	200 ± 16	29.5 ± 3.1	789 ± 57	204 ± 15
QCD	12.9 ± 5.4	1.05 ± 0.55	14.5 ± 4.6	7.2 ± 3.9
Total bkg.	1170 ± 100	699 ± 72	1077 ± 70	345 ± 23
Data	1152	710	1062	335

Figure 4: Distributions of $\min[M(\ell,b)]$ in the $t\bar{t}$ control region, for 1 b-tagged jet (upper left) and $\geq$2 b-tagged jets (upper right) categories, and of $\min[M(\ell,j)]$ in the W+jets control region, for 0 W-tagged jets (lower left) and $\geq$1 W-tagged jets (lower right) categories. Example signal distributions are also shown. The background distributions correspond to background-only fit to data while signal distributions are before the fit to data. Electron and muon event samples are combined. The last bin includes overflow events and its content is divided by the bin width. The distributions in each category have variable-size bins, chosen so that the statistical uncertainty in the total background in each bin is less than 30%. The lower panel in each plot shows the difference between the observed and the predicted numbers of events in that bin divided by the total uncertainty. The total uncertainty is calculated as the sum in quadrature of the statistical uncertainty in the observed measurement and the statistical and systematic uncertainties in the background-only fit to data.

7.2 Event yields and template distributions

In the single-lepton signal region, the LH (RH) signal efficiencies range between 4.1 (5.0) and 13.1 (14.7)%. Events in the signal region are separated into 16 categories based on the flavor of the lepton (e, μ), the number of b-tagged jets (1, $\geq$2), the number of W-tagged jets (0, $\geq$1), and the number of t-tagged jets (0, $\geq$1). Event yields for each analysis category are given in Table 3 after a background-only fit to data with the contribution from the electron and muon channels combined. Figure 5 shows the distribution for $\min[M(\ell, b)]$ for events with zero t-tagged jets, while Fig. 6 shows the $\min[M(\ell, b)]$ distribution for events with at least one t-tagged jet, both of which are shown after a background-only fit to data. The distributions are separated for each analysis category, but again the electron and muon channels are combined. No significant discrepancy is seen between the observed and predicted $\min[M(\ell, b)]$ distributions.

Table 3: Expected (observed) numbers of background (data) events passing the final selection requirements, in the signal region ($\Delta R(\ell, j_2) > 1.0$) categories, after combining the single-electron and single-muon channels. The numbers of events expected from two example signals are also shown. The event yields and their uncertainties correspond to the background-only fit to data for the background, while for the signal they are based on the values before the fit to data.

Sample	0 t, 0 W, 1 b	0 t, 0 W, $\geq$2 b	0 t, $\geq$1 W, 1 b	0 t, $\geq$1 W, $\geq$2 b
LH $X_{5/3}$ (0.9 TeV)	5.6 ± 1.3	4.9 ± 1.2	43.6 ± 2.3	36.5 ± 2.3
RH $X_{5/3}$ (1.2 TeV)	1.13 ± 0.30	0.85 ± 0.24	10.44 ± 0.66	7.67 ± 0.56
TOP	545 ± 49	334 ± 32	462 ± 44	306 ± 30
EWK	366 ± 27	54.0 ± 4.7	108.5 ± 9.3	19.7 ± 2.7
QCD	24.6 ± 7.6	7.9 ± 3.7	7.6 ± 4.4	$0.65 \pm^{0.71}_{0.65}$
Total bkg.	935 ± 62	396 ± 33	578 ± 47	327 ± 30
Data	984	416	577	321
Sample	$\geq$1 t, 0 W, 1 b	$\geq$1 t, 0 W, $\geq$2 b	$\geq$1 t, $\geq$1 W, 1 b	$\geq$1 t, $\geq$1 W, $\geq$2 b
LH $X_{5/3}$ (0.9 TeV)	17.6 ± 1.6	15.5 ± 1.5	39.7 ± 2.3	34.5 ± 2.2
RH $X_{5/3}$ (1.2 TeV)	4.16 ± 0.52	3.40 ± 0.49	13.82 ± 0.84	11.83 ± 0.82
TOP	367 ± 41	267 ± 31	139 ± 16	108 ± 13
EWK	108.7 ± 9.0	19.3 ± 1.8	22.6 ± 3.6	2.69 ± 0.31
QCD	6.6 ± 2.4	1.41 ± 0.65	1.36 ± 0.66	0.47 ± 0.32
Total bkg.	482 ± 44	287 ± 31	163 ± 17	111 ± 13
Data	465	285	135	123

8 Systematic uncertainties

The uncertainties in the lepton reconstruction, identification, and isolation efficiencies are derived from the uncertainties in the data-to-simulation scale factors and range from 1 to 3%. These uncertainties are applied per lepton. A 2.5% uncertainty is assigned to the integrated luminosity measurement [56] used to scale the simulated signal and background processes. The above uncertainties only affect the normalization of the simulated processes and not their shape.

Both final states have uncertainties in their simulation-based predictions from the uncertainties in the lepton triggering efficiency, the jet energy scale (JES), the jet energy resolution (JER), the pileup modeling, the cross section normalization, and the choice of PDFs. For the same-sign
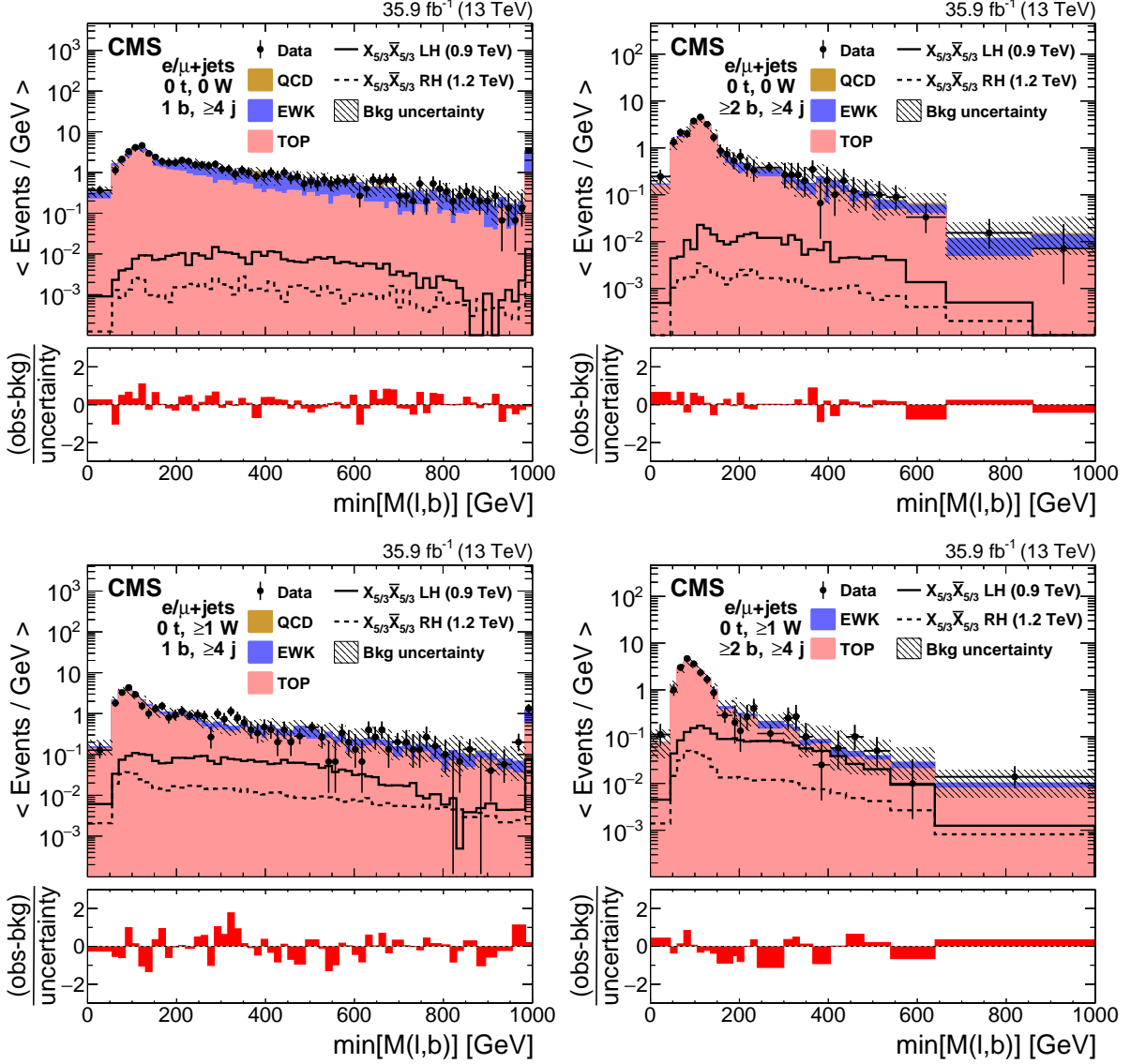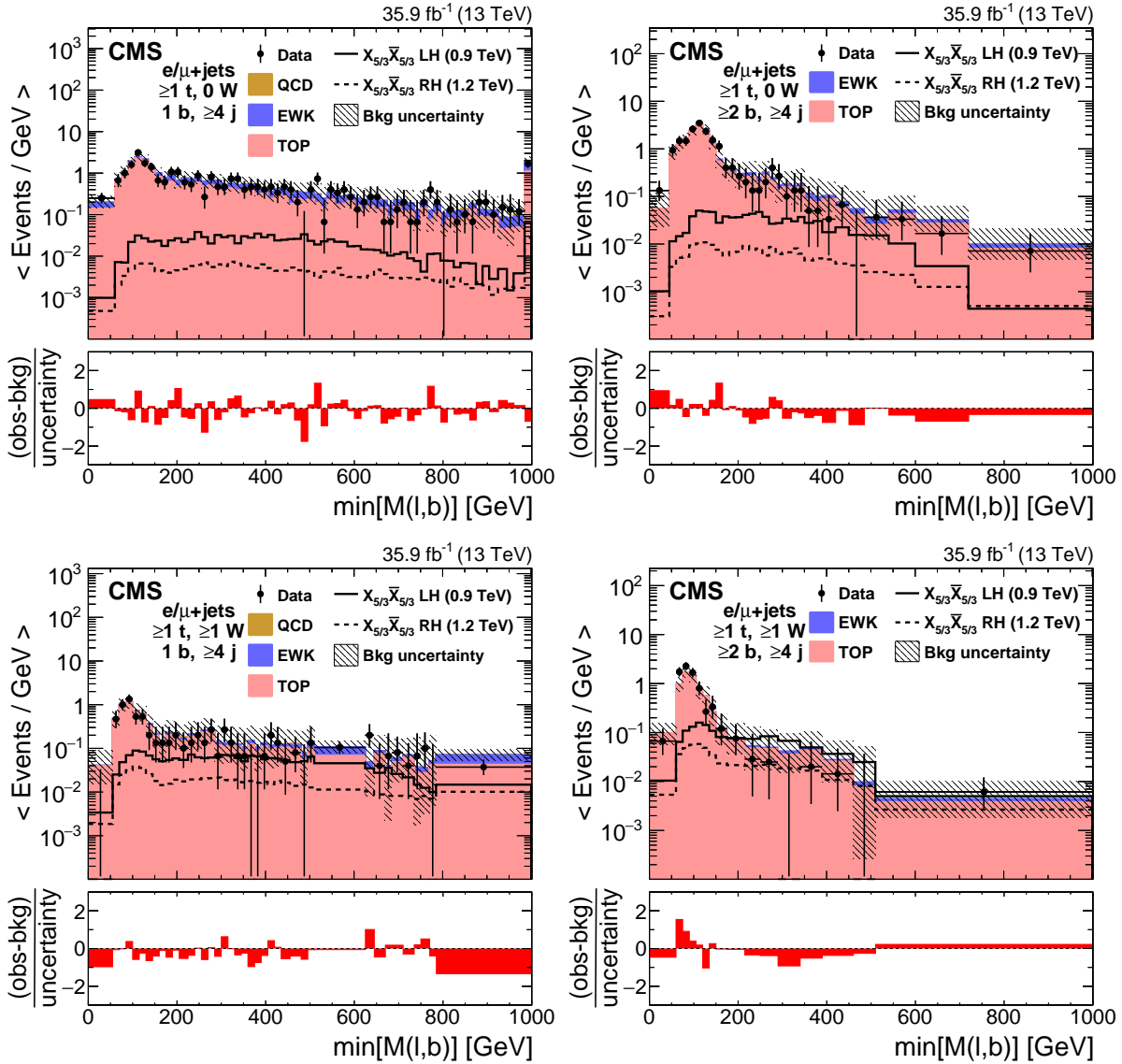
Figure 5: Distributions of $\min[M(\ell, b)]$ in events with 0 t-tagged jets, 0 (upper) or ≥ 1 (lower) W-tagged jets, and 1 (left) or ≥ 2 (right) b-tagged jets for the combined electron and muon samples in the signal region. Example signal distributions are also shown. The background distributions correspond to the background-only fit to data, while signal distributions are before the fit to data. The last bin includes overflow events and its content is divided by the bin width. The distributions in each category have variable-size bins, chosen so that the statistical uncertainty in the total background in each bin is less than 30%. The lower panel in each plot shows the difference between the observed and the predicted numbers of events in that bin divided by the total uncertainty. The total uncertainty is calculated as the sum in quadrature of the statistical uncertainty in the observed measurement and the statistical and systematic uncertainties in the background-only fit to data.

Figure 6: Distributions of $\min[M(\ell, b)]$ in events with ≥ 1 t-tagged jets, 0 (upper) or ≥ 1 (lower) W-tagged jets, and 1 (left) or ≥ 2 (right) b-tagged jets for the combined electron and muon samples in the signal region. Example signal distributions are also shown. The background distributions correspond to the background-only fit to data, while signal distributions are before the fit to data. The last bin includes overflow events and its content is divided by the bin width. The distributions in each category have variable-size bins, chosen so that the statistical uncertainty in the total background in each bin is less than 30%. The lower panel in each plot shows the difference between the observed and the predicted numbers of events in that bin divided by the total uncertainty. The total uncertainty is calculated as the sum in quadrature of the statistical uncertainty in the observed measurement and the statistical and systematic uncertainties in the background-only fit to data.

dilepton final state, the uncertainty in the lepton triggering efficiency is 3% while for the single-lepton final state it ranges between 2 and 5%. In both final states, this uncertainty is applied per event. The JES and JER uncertainties are estimated by varying the relevant parameters up and down by one standard deviation (s.d.) and repeating the analysis selections. The pileup uncertainty is assessed by varying the total inelastic cross section ($\sigma_{inel.}$) used in the pileup reweighting by $\pm 4.6\%$ [57]. The uncertainty in the theoretical cross section from renormalization and factorization energy scales is estimated by independently varying the scales up and down by a factor of two and taking the maximum variation as the uncertainty. The uncertainty associated with the PDFs used for the MC generation is evaluated from the set of NNPDF3.0 fitted replicas, following the standard procedure [32].

The single-lepton final state considers the shape variations in the signal distributions that come from varying the renormalization and factorization scales and the choice of PDF set. For the same-sign dilepton final state, only their effect on the signal acceptance is considered, since a "cut-and-count" analysis is used in this case. The normalization changes due to the variations in the signal acceptance are found to be negligible in the single-lepton final state. The details of the systematic uncertainties are shown in Table 4 for the same-sign dilepton final state and in Table 5 for the single-lepton final state.

Table 4: Systematic uncertainties in percentage (%) in the same-sign dilepton final state, associated with the simulated processes. The "Normalization" column refers to the uncertainties from the cross section normalization and the choice of PDF set.

Process	JES	JER	Pileup	Normalization
$t\bar{t}W$	3	2	4	19
$t\bar{t}Z$	3	2	4	12
$t\bar{t}H$	3	2	4	30
$t\bar{t}t\bar{t}$	2	2	4	50
WZ	9	2	4	24
ZZ	4	2	4	10
WW	9	2	4	50
WWZ	9	2	4	50
WZZ	9	2	4	50
ZZZ	9	2	4	50
$X_{5/3}$	3	1	1	—

In the single-lepton final state, uncertainties are also applied for the corrections on the b tagging, light quark mistagging, W tagging, and t tagging scale factors. The W tagging uncertainties have different components, which are treated as uncorrelated: corrections to the groomed mass scale and smearing, τ_2/τ_1 selection efficiency, and its p_T dependence. For the top quark p_T reweighting, the difference between the weighted and unweighted distributions is added as a one-sided systematic uncertainty.

Lastly, in the same-sign dilepton final state, there are uncertainties in the predictions of background processes whose estimates are made using control samples in data. As stated above, a 30% uncertainty is assigned to the predicted yield of background events from charge misidentification, and a 50% uncertainty is assigned to the predicted yield of background events from processes with nonprompt leptons.

Systematic uncertainties that have the same source for the two different final states (e.g. the uncertainty in the lepton identification) are treated as fully correlated between the two final states.

Table 5: Summary of systematic uncertainties in the single-lepton final state. These uncertainties are included in both signal and all background processes, except for the top p_T systematic uncertainty, which is included only in $t\bar{t}$. The range of uncertainty values in percentage (%) corresponds to the effect on the yields before the fit to data and is given across the relevant background processes and channels for each systematic uncertainty.

Source	Uncertainty range
Trigger efficiency	2–5
Jet energy scale	0.5–52
Jet energy resolution	0–3
b/c tagging	0–5
udsg mistagging	0–4
W tagging: mass resolution	0–13
W tagging: mass scale	0–21
W tagging: τ_2/τ_1	0–2
W tagging: τ_2/τ_1 extrapolation	0–2
t tagging	0–4
Top p_T	0–19
Pileup	0–4
PDF	2–9
QCD renorm./fact. scale	12–36

9 Results

No significant excess of events is observed above the SM prediction. Upper limits at 95% CL are set on the production cross sections $pp \rightarrow X_{5/3}\overline{X}_{5/3}$ for both couplings and for the different final states, as well as for their combination. Bayesian statistics [58, 59] are used to calculate observed and expected limits with a flat prior taken for the signal cross section. The same-sign dilepton final state limits are based on a counting experiment, while in the single-lepton final state, a binned likelihood fit on the distributions of $\min[M(\ell, b)]$ is performed simultaneously in the signal and control regions. Systematic uncertainties are treated as nuisance parameters with normalization uncertainties having a log-normal prior and shape uncertainties a Gaussian prior. The fit does not change any nuisance parameter by a significant amount compared to its pre-fit value. After the full analysis selection described above, lower observed (expected) limits of 1.16 (1.20) and 1.10 (1.16) TeV are placed on the mass of the $X_{5/3}$ particle with RH and LH couplings to W bosons, respectively, using the same-sign dilepton final state. In the single-lepton final state, observed (expected) limits of 1.32 (1.23) and 1.30 (1.23) TeV are placed on the mass of the $X_{5/3}$ particle with RH and LH couplings to W bosons, respectively. Combining the two final states yields a lower observed (expected) limit on the $X_{5/3}$ mass of 1.33 (1.30) TeV for an $X_{5/3}$ particle with RH couplings to W bosons and 1.30 (1.28) TeV for an $X_{5/3}$ particle with LH couplings to W bosons. Figure 7 shows the limits for the individual final states, while Fig. 8 shows the limits obtained by combining the two final states.

10 Summary

A search has been performed for a heavy top quark partner with an exotic 5/3 charge ($X_{5/3}$) using proton-proton collision data collected by the CMS experiment in 2016 at a center-of-mass energy of 13 TeV and corresponding to $35.9\,\text{fb}^{-1}$. The $X_{5/3}$ quark is assumed always to decay into a top quark and a W boson. Two different final states, same-sign dilepton and single-lepton, are analyzed separately and then combined. No significant excess over the expected
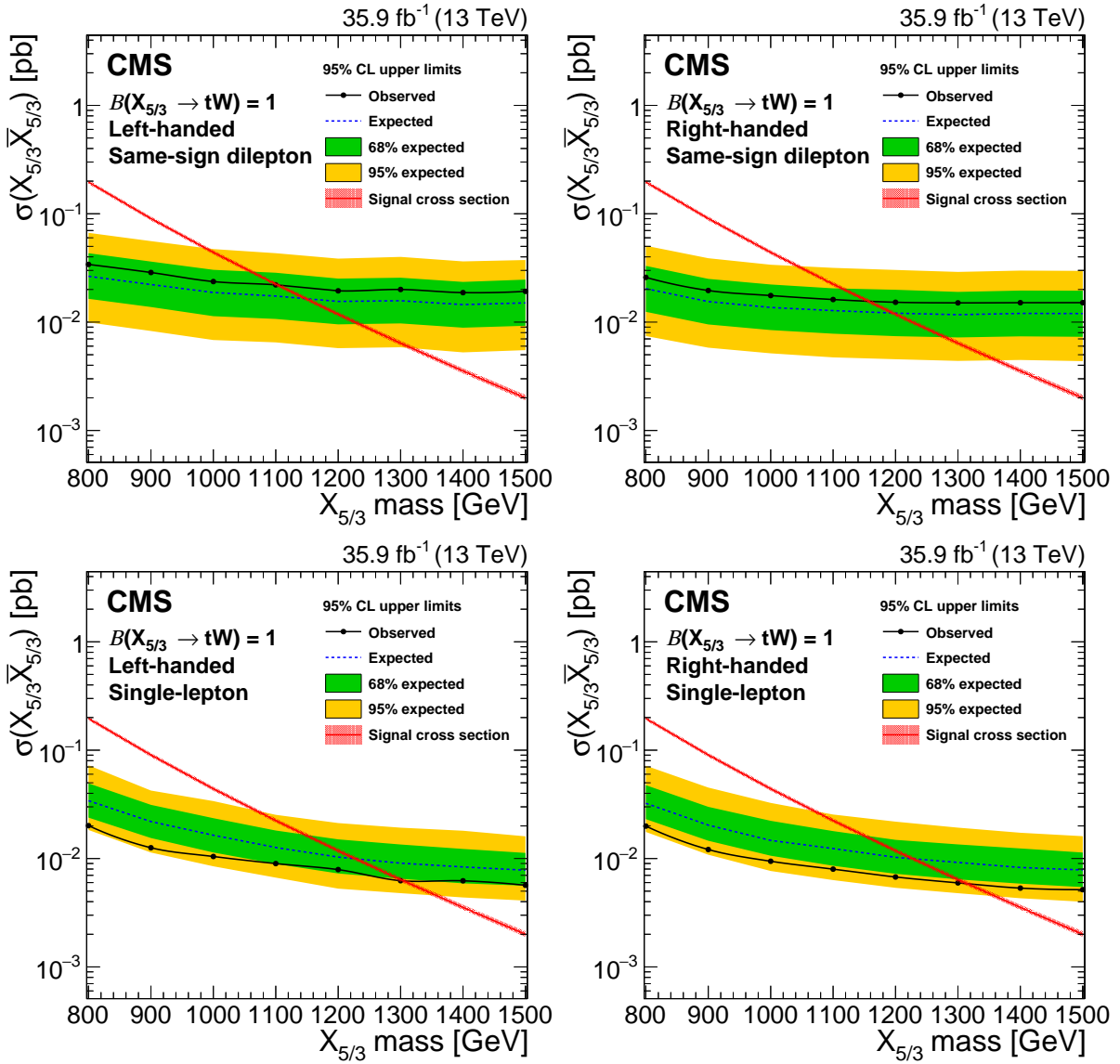
Figure 7: Expected and observed limits at 95% CL for an LH (left) and RH (right) $X_{5/3}$ after combining all categories for the same-sign dilepton (upper row) and the single-lepton (lower row) final states. The theoretical uncertainty in the signal cross section is shown as a narrow band around the theoretical prediction.
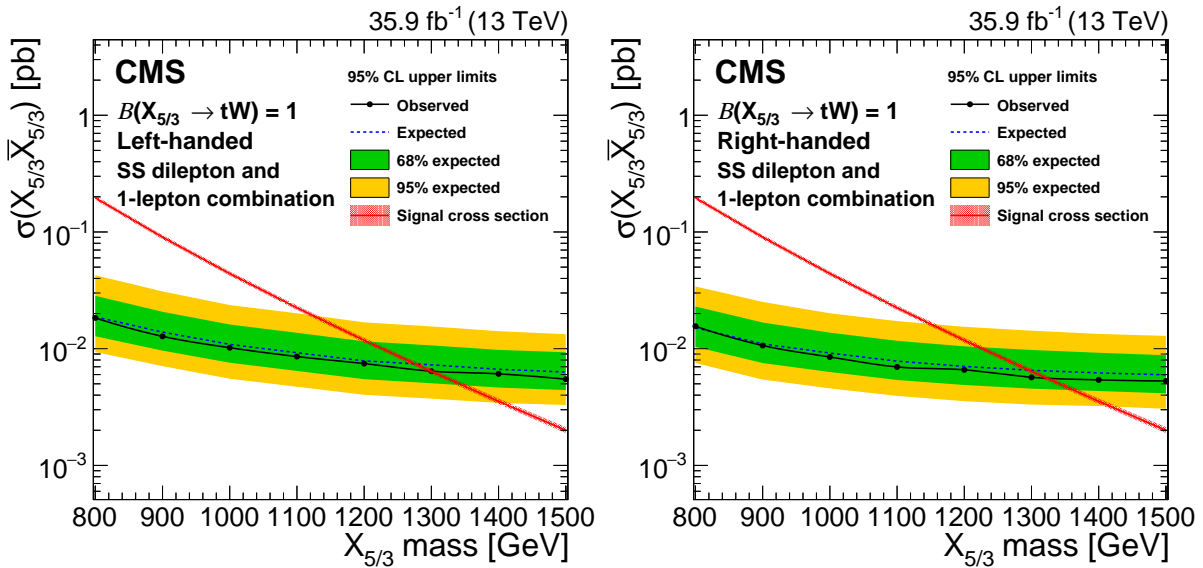
Figure 8: Expected and observed limits at 95% CL for an LH (left) and RH (right) $X_{5/3}$ after combining the same-sign dilepton and single-lepton final states. The theoretical uncertainty in the signal cross section is shown as a narrow band around the theoretical prediction.

standard model backgrounds is seen in data. Lower limits are set on the mass of the $X_{5/3}$ particle. The observed (expected) limit is 1.33 (1.30) TeV for an $X_{5/3}$ particle with right-handed couplings to W bosons and 1.30 (1.28) TeV for an $X_{5/3}$ particle with left-handed couplings to W bosons in a combination of the same-sign dilepton and single-lepton final states.

Acknowledgments

References

[1] R. Contino and G. Servant, "Discovering the top partners at the LHC using same-sign dilepton final states", *JHEP* **06** (2008) 026, `doi:10.1088/1126-6708/2008/06/026`, `arXiv:0801.1679`.

[2] A. De Simone, O. Matsedonskyi, R. Rattazzi, and A. Wulzer, "A first top partner hunter's guide", *JHEP* **04** (2013) 004, `doi:10.1007/JHEP04(2013)004`, `arXiv:1211.5663`.

[3] K. Agashe, R. Contino, and A. Pomarol, "The minimal composite Higgs model", *Nucl. Phys. B* **719** (2005) 165, `doi:10.1016/j.nuclphysb.2005.04.035`, `arXiv:hep-ph/0412089`.

[4] D. B. Kaplan, "Flavor at SSC energies: A new mechanism for dynamically generated fermion masses", *Nucl. Phys. B* **365** (1991) 259, `doi:10.1016/S0550-3213(05)80021-5`.

[5] A. Azatov and J. Galloway, "Light custodians and Higgs physics in composite models", *Phys. Rev. D* **85** (2012) 055013, `doi:10.1103/PhysRevD.85.055013`, `arXiv:1110.5646`.

[6] G. Cacciapaglia et al., "Heavy vector-like quark with charge 5/3 at the LHC", *JHEP* **03** (2013) 004, `doi:10.1007/JHEP03(2013)004`, `arXiv:1211.4034`.

[7] CMS Collaboration, "Search for top-quark partners with charge 5/3 in the same-sign dilepton final state", *Phys. Rev. Lett.* **112** (2014) 171801, `doi:10.1103/PhysRevLett.112.171801`, `arXiv:1312.2391`.

[8] CMS Collaboration, "Search for top quark partners with charge 5/3 in proton-proton collisions at $\sqrt{s} = 13$ TeV", *JHEP* **08** (2017) 073, `doi:10.1007/JHEP08(2017)073`, `arXiv:1705.10967`.

[9] ATLAS Collaboration, "Analysis of events with *b*-jets and a pair of leptons of the same charge in *pp* collisions at $\sqrt{s} = 8$ TeV with the ATLAS detector", *JHEP* **10** (2015) 150, doi:10.1007/JHEP10(2015)150, arXiv:1504.04605.

[10] ATLAS Collaboration, "Search for vector-like *B* quarks in events with one isolated lepton, missing transverse momentum and jets at $\sqrt{s} = 8$ TeV with the ATLAS detector", *Phys. Rev. D* **91** (2015) 112011, doi:10.1103/PhysRevD.91.112011, arXiv:1503.05425.

[11] ATLAS Collaboration, "Search for pair production of heavy vector-like quarks decaying to high-p_T W bosons and b quarks in the lepton-plus-jets final state in pp collisions at $\sqrt{s} = 13$ TeV with the ATLAS detector", *JHEP* **10** (2017) 141, doi:10.1007/JHEP10(2017)141, arXiv:1707.03347.

[12] ATLAS Collaboration, "Search for pair production of heavy vector-like quarks decaying into high-p_T W bosons and top quarks in the lepton-plus-jets final state in *pp* collisions at $\sqrt{s} = 13$ TeV with the ATLAS detector", *JHEP* **08** (2018) 048, doi:10.1007/JHEP08(2018)048, arXiv:1806.01762.

[13] ATLAS Collaboration, "Search for new phenomena in events with same-charge leptons and *b*-jets in *pp* collisions at $\sqrt{s} = 13$ TeV with the ATLAS detector", *JHEP* **12** (2018) 039, doi:10.1007/JHEP12(2018)039, arXiv:1807.11883.

[14] ATLAS Collaboration, "Combination of the searches for pair-produced vector-like partners of the third-generation quarks at $\sqrt{s} = 13$ TeV with the ATLAS detector", *Phys. Rev. Lett.* **121** (2018) 211801, doi:10.1103/PhysRevLett.121.211801, arXiv:1808.02343.

[15] CMS Collaboration, "The CMS trigger system", *JINST* **12** (2017) P01020, doi:10.1088/1748-0221/12/01/P01020, arXiv:1609.02366.

[16] CMS Collaboration, "The CMS experiment at the CERN LHC", *JINST* **3** (2008) S08004, doi:10.1088/1748-0221/3/08/S08004.

[17] J. Alwall et al., "The automated computation of tree-level and next-to-leading order differential cross sections, and their matching to parton shower simulations", *JHEP* **07** (2014) 079, doi:10.1007/JHEP07(2014)079, arXiv:1405.0301.

[18] P. Artoisenet, R. Frederix, O. Mattelaer, and R. Rietkerk, "Automatic spin-entangled decays of heavy resonances in Monte Carlo simulations", *JHEP* **03** (2013) 015, doi:10.1007/JHEP03(2013)015, arXiv:1212.3460.

[19] M. Czakon and A. Mitov, "Top++: a program for the calculation of the top-pair cross-section at hadron colliders", *Comput. Phys. Commun.* **185** (2014) 2930, doi:10.1016/j.cpc.2014.06.021, arXiv:1112.5675.

[20] M. Czakon, P. Fiedler, and A. Mitov, "The total top quark pair production cross-section at hadron colliders through $\mathcal{O}(\alpha_S^4)$", *Phys. Rev. Lett.* **110** (2013) 252004, doi:10.1103/PhysRevLett.110.252004, arXiv:1303.6254.

[21] M. Czakon and A. Mitov, "NNLO corrections to top-pair production at hadron colliders: the all-fermionic scattering channels", *JHEP* **12** (2012) 054, doi:10.1007/JHEP12(2012)054, arXiv:1207.0236.

[22] M. Czakon and A. Mitov, "NNLO corrections to top pair production at hadron colliders: the quark-gluon reaction", *JHEP* **01** (2013) 080, `doi:10.1007/JHEP01(2013)080`, `arXiv:1210.6832`.

[23] P. Bärnreuther, M. Czakon, and A. Mitov, "Percent level precision physics at the Tevatron: first genuine NNLO QCD corrections to $q\bar{q} \to t\bar{t} + X$", *Phys. Rev. Lett.* **109** (2012) 132001, `doi:10.1103/PhysRevLett.109.132001`, `arXiv:1204.5201`.

[24] M. Cacciari et al., "Top-pair production at hadron colliders with next-to-next-to-leading logarithmic soft-gluon resummation", *Phys. Lett. B* **710** (2012) 612, `doi:10.1016/j.physletb.2012.03.013`, `arXiv:1111.5869`.

[25] P. Nason, "A new method for combining NLO QCD with shower Monte Carlo algorithms", *JHEP* **11** (2004) 040, `doi:10.1088/1126-6708/2004/11/040`, `arXiv:hep-ph/0409146`.

[26] S. Frixione, P. Nason, and C. Oleari, "Matching NLO QCD computations with parton shower simulations: the POWHEG method", *JHEP* **11** (2007) 070, `doi:10.1088/1126-6708/2007/11/070`, `arXiv:0709.2092`.

[27] S. Alioli, P. Nason, C. Oleari, and E. Re, "A general framework for implementing NLO calculations in shower Monte Carlo programs: the POWHEG BOX", *JHEP* **06** (2010) 043, `doi:10.1007/JHEP06(2010)043`, `arXiv:1002.2581`.

[28] S. Frixione, P. Nason, and G. Ridolfi, "A positive-weight next-to-leading-order Monte Carlo for heavy flavour hadroproduction", *JHEP* **09** (2007) 126, `doi:10.1088/1126-6708/2007/09/126`, `arXiv:0707.3088`.

[29] J. Alwall et al., "Comparative study of various algorithms for the merging of parton showers and matrix elements in hadronic collisions", *Eur. Phys. J. C* **53** (2008) 473, `doi:10.1140/epjc/s10052-007-0490-5`, `arXiv:0706.2569`.

[30] R. Frederix and S. Frixione, "Merging meets matching in MC@NLO", *JHEP* **12** (2012) 061, `doi:10.1007/JHEP12(2012)061`, `arXiv:1209.6215`.

[31] T. Sjöstrand et al., "An introduction to PYTHIA 8.2", *Comput. Phys. Commun.* **191** (2015) 159, `doi:10.1016/j.cpc.2015.01.024`, `arXiv:1410.3012`.

[32] NNPDF Collaboration, "Parton distributions for the LHC Run II", *JHEP* **04** (2015) 040, `doi:10.1007/JHEP04(2015)040`, `arXiv:1410.8849`.

[33] CMS Collaboration, "Event generator tunes obtained from underlying event and multiparton scattering measurements", *Eur. Phys. J. C* **76** (2016) 155, `doi:10.1140/epjc/s10052-016-3988-x`, `arXiv:1512.00815`.

[34] P. Skands, S. Carrazza, and J. Rojo, "Tuning PYTHIA 8.1: the Monash 2013 tune", *Eur. Phys. J. C* **74** (2014) 3024, `doi:10.1140/epjc/s10052-014-3024-y`, `arXiv:1404.5630`.

[35] CMS Collaboration, "Investigations of the impact of the parton shower tuning in Pythia 8 in the modelling of $t\bar{t}$ at $\sqrt{s} = 8$ and 13 TeV", CMS Physics Analysis Summary CMS-PAS-TOP-16-021, 2016.

[36] GEANT4 Collaboration, "GEANT4—a simulation toolkit", *Nucl. Instrum. Meth. A* **506** (2003) 250, `doi:10.1016/S0168-9002(03)01368-8`.

[37] CMS Collaboration, "Measurement of the differential cross section for top quark pair production in pp collisions at $\sqrt{s} = 8$ TeV", *Eur. Phys. J. C* **75** (2015) 542, `doi:10.1140/epjc/s10052-015-3709-x`, `arXiv:1505.04480`.

[38] CMS Collaboration, "Particle-flow reconstruction and global event description with the CMS detector", *JINST* **12** (2017) P10003, `doi:10.1088/1748-0221/12/10/P10003`, `arXiv:1706.04965`.

[39] M. Cacciari, G. P. Salam, and G. Soyez, "The anti-k_T jet clustering algorithm", *JHEP* **04** (2008) 063, `doi:10.1088/1126-6708/2008/04/063`, `arXiv:0802.1189`.

[40] M. Cacciari, G. P. Salam, and G. Soyez, "FastJet user manual", *Eur. Phys. J. C* **72** (2012) 1896, `doi:10.1140/epjc/s10052-012-1896-2`, `arXiv:1111.6097`.

[41] CMS Collaboration, "Performance of electron reconstruction and selection with the CMS detector in proton-proton collisions at $\sqrt{s} = 8$ TeV", *JINST* **10** (2015) P06005, `doi:10.1088/1748-0221/10/06/P06005`, `arXiv:1502.02701`.

[42] CMS Collaboration, "CMS tracking performance results from early LHC operation", *Eur. Phys. J. C* **70** (2010) 1165, `doi:10.1140/epjc/s10052-010-1491-3`, `arXiv:1007.1988`.

[43] W. Adam, R. Frühwirth, A. Strandlie, and T. Todorov, "Reconstruction of electrons with the Gaussian-sum filter in the CMS tracker at the LHC", *J. Phys. G* **31** (2005) N9, `doi:10.1088/0954-3899/31/9/N01`, `arXiv:physics/0306087`.

[44] M. Cacciari and G. P. Salam, "Pileup subtraction using jet areas", *Phys. Lett. B* **659** (2008) 119, `doi:10.1016/j.physletb.2007.09.077`, `arXiv:0707.1378`.

[45] CMS Collaboration, "Measurement of the inclusive W and Z production cross sections in pp collisions at $\sqrt{s} = 7$ TeV", *JHEP* **10** (2011) 132, `doi:10.1007/JHEP10(2011)132`, `arXiv:1107.4789`.

[46] M. Cacciari, G. P. Salam, and G. Soyez, "The catchment area of jets", *JHEP* **04** (2008) 005, `doi:10.1088/1126-6708/2008/04/005`, `arXiv:0802.1188`.

[47] CMS Collaboration, "Jet algorithms performance in 13 TeV data", CMS Physics Analysis Summary CMS-PAS-JME-16-003, 2017.

[48] CMS Collaboration, "Determination of jet energy calibration and transverse momentum resolution in CMS", *JINST* **6** (2011) P11002, `doi:10.1088/1748-0221/6/11/P11002`, `arXiv:1107.4277`.

[49] CMS Collaboration, "Jet energy scale and resolution in the CMS experiment in pp collisions at 8 TeV", *JINST* **12** (2017) P02014, `doi:10.1088/1748-0221/12/02/P02014`, `arXiv:1607.03663`.

[50] CMS Collaboration, "Identification of heavy-flavour jets with the CMS detector in pp collisions at 13 TeV", *JINST* **13** (2018) P05011, `doi:10.1088/1748-0221/13/05/P05011`, `arXiv:1712.07158`.

[51] A. J. Larkoski, S. Marzani, G. Soyez, and J. Thaler, "Soft drop", *JHEP* **05** (2014) 146, `doi:10.1007/JHEP05(2014)146`, `arXiv:1402.2657`.

[52] J. Thaler and K. Van Tilburg, "Maximizing boosted top identification by minimizing *N*-subjettiness", *JHEP* **02** (2012) 093, `doi:10.1007/JHEP02(2012)093`, `arXiv:1108.2701`.

[53] S. D. Ellis, C. K. Vermilion, and J. R. Walsh, "Techniques for improved heavy particle searches with jet substructure", *Phys. Rev. D* **80** (2009) 051501, `doi:10.1103/PhysRevD.80.051501`, `arXiv:0903.5081`.

[54] CMS Collaboration, "Search for new physics in same-sign dilepton events in proton-proton collisions at $\sqrt{s} = 13$ TeV", *Eur. Phys. J. C* **76** (2016) 439, `doi:10.1140/epjc/s10052-016-4261-z`, `arXiv:1605.03171`.

[55] CMS Collaboration, "Search for new physics with same-sign isolated dilepton events with jets and missing transverse energy at the LHC", *JHEP* **06** (2011) 077, `doi:10.1007/JHEP06(2011)077`, `arXiv:1104.3168`.

[56] CMS Collaboration, "CMS luminosity measurement for the 2016 data-taking period", CMS Physics Analysis Summary CMS-PAS-LUM-17-001, 2017.

[57] CMS Collaboration, "Measurement of the inelastic proton-proton cross section at $\sqrt{s} = 13$ TeV", *JHEP* **07** (2018) 161, `doi:10.1007/JHEP07(2018)161`, `arXiv:1802.02613`.

[58] Particle Data Group, M. Tanabashi et al., "Review of particle physics", *Phys. Rev. D* **98** (2018) 030001, `doi:10.1103/PhysRevD.98.030001`. See Ch. 39, "Statistics", G. Cowan.

[59] J. Ott, "THETA—A framework for template-based modeling and inference", 2010. `http://www-ekp.physik.uni-karlsruhe.de/~ott/theta/theta-auto`.

A The CMS Collaboration

Yerevan Physics Institute, Yerevan, Armenia
A.M. Sirunyan, A. Tumasyan

Institut für Hochenergiephysik, Wien, Austria
W. Adam, F. Ambrogi, E. Asilar, T. Bergauer, J. Brandstetter, M. Dragicevic, J. Erö, A. Escalante Del Valle, M. Flechl, R. Frühwirth[1], V.M. Ghete, J. Hrubec, M. Jeitler[1], N. Krammer, I. Krätschmer, D. Liko, T. Madlener, I. Mikulec, N. Rad, H. Rohringer, J. Schieck[1], R. Schöfbeck, M. Spanring, D. Spitzbart, A. Taurok, W. Waltenberger, J. Wittmann, C.-E. Wulz[1], M. Zarucki

Institute for Nuclear Problems, Minsk, Belarus
V. Chekhovsky, V. Mossolov, J. Suarez Gonzalez

Universiteit Antwerpen, Antwerpen, Belgium
E.A. De Wolf, D. Di Croce, X. Janssen, J. Lauwers, M. Pieters, M. Van De Klundert, H. Van Haevermaet, P. Van Mechelen, N. Van Remortel

Vrije Universiteit Brussel, Brussel, Belgium
S. Abu Zeid, F. Blekman, J. D'Hondt, I. De Bruyn, J. De Clercq, K. Deroover, G. Flouris, D. Lontkovskyi, S. Lowette, I. Marchesini, S. Moortgat, L. Moreels, Q. Python, K. Skovpen, S. Tavernier, W. Van Doninck, P. Van Mulders, I. Van Parijs

Université Libre de Bruxelles, Bruxelles, Belgium
D. Beghin, B. Bilin, H. Brun, B. Clerbaux, G. De Lentdecker, H. Delannoy, B. Dorney, G. Fasanella, L. Favart, R. Goldouzian, A. Grebenyuk, A.K. Kalsi, T. Lenzi, J. Luetic, N. Postiau, E. Starling, L. Thomas, C. Vander Velde, P. Vanlaer, D. Vannerom, Q. Wang

Ghent University, Ghent, Belgium
T. Cornelis, D. Dobur, A. Fagot, M. Gul, I. Khvastunov[2], D. Poyraz, C. Roskas, D. Trocino, M. Tytgat, W. Verbeke, B. Vermassen, M. Vit, N. Zaganidis

Université Catholique de Louvain, Louvain-la-Neuve, Belgium
H. Bakhshiansohi, O. Bondu, S. Brochet, G. Bruno, C. Caputo, P. David, C. Delaere, M. Delcourt, B. Francois, A. Giammanco, G. Krintiras, V. Lemaitre, A. Magitteri, A. Mertens, M. Musich, K. Piotrzkowski, A. Saggio, M. Vidal Marono, S. Wertz, J. Zobec

Centro Brasileiro de Pesquisas Fisicas, Rio de Janeiro, Brazil
F.L. Alves, G.A. Alves, L. Brito, M. Correa Martins Junior, G. Correia Silva, C. Hensel, A. Moraes, M.E. Pol, P. Rebello Teles

Universidade do Estado do Rio de Janeiro, Rio de Janeiro, Brazil
E. Belchior Batista Das Chagas, W. Carvalho, J. Chinellato[3], E. Coelho, E.M. Da Costa, G.G. Da Silveira[4], D. De Jesus Damiao, C. De Oliveira Martins, S. Fonseca De Souza, H. Malbouisson, D. Matos Figueiredo, M. Melo De Almeida, C. Mora Herrera, L. Mundim, H. Nogima, W.L. Prado Da Silva, L.J. Sanchez Rosas, A. Santoro, A. Sznajder, M. Thiel, E.J. Tonelli Manganote[3], F. Torres Da Silva De Araujo, A. Vilela Pereira

Universidade Estadual Paulista [a], Universidade Federal do ABC [b], São Paulo, Brazil
S. Ahuja[a], C.A. Bernardes[a], L. Calligaris[a], T.R. Fernandez Perez Tomei[a], E.M. Gregores[b], P.G. Mercadante[b], S.F. Novaes[a], SandraS. Padula[a], D. Romero Abad[b]

Institute for Nuclear Research and Nuclear Energy, Bulgarian Academy of Sciences, Sofia,

Bulgaria
A. Aleksandrov, R. Hadjiiska, P. Iaydjiev, A. Marinov, M. Misheva, M. Rodozov, M. Shopova, G. Sultanov

University of Sofia, Sofia, Bulgaria
A. Dimitrov, L. Litov, B. Pavlov, P. Petkov

Beihang University, Beijing, China
W. Fang[5], X. Gao[5], L. Yuan

Institute of High Energy Physics, Beijing, China
M. Ahmad, J.G. Bian, G.M. Chen, H.S. Chen, M. Chen, Y. Chen, C.H. Jiang, D. Leggat, H. Liao, Z. Liu, F. Romeo, S.M. Shaheen[6], A. Spiezia, J. Tao, C. Wang, Z. Wang, E. Yazgan, H. Zhang, J. Zhao

State Key Laboratory of Nuclear Physics and Technology, Peking University, Beijing, China
Y. Ban, G. Chen, A. Levin, J. Li, L. Li, Q. Li, Y. Mao, S.J. Qian, D. Wang, Z. Xu

Tsinghua University, Beijing, China
Y. Wang

Universidad de Los Andes, Bogota, Colombia
C. Avila, A. Cabrera, C.A. Carrillo Montoya, L.F. Chaparro Sierra, C. Florez, C.F. González Hernández, M.A. Segura Delgado

University of Split, Faculty of Electrical Engineering, Mechanical Engineering and Naval Architecture, Split, Croatia
B. Courbon, N. Godinovic, D. Lelas, I. Puljak, T. Sculac

University of Split, Faculty of Science, Split, Croatia
Z. Antunovic, M. Kovac

Institute Rudjer Boskovic, Zagreb, Croatia
V. Brigljevic, D. Ferencek, K. Kadija, B. Mesic, A. Starodumov[7], T. Susa

University of Cyprus, Nicosia, Cyprus
M.W. Ather, A. Attikis, M. Kolosova, G. Mavromanolakis, J. Mousa, C. Nicolaou, F. Ptochos, P.A. Razis, H. Rykaczewski

Charles University, Prague, Czech Republic
M. Finger[8], M. Finger Jr.[8]

Escuela Politecnica Nacional, Quito, Ecuador
E. Ayala

Universidad San Francisco de Quito, Quito, Ecuador
E. Carrera Jarrin

Academy of Scientific Research and Technology of the Arab Republic of Egypt, Egyptian Network of High Energy Physics, Cairo, Egypt
A. Ellithi Kamel[9], A. Mahrous[10], Y. Mohammed[11]

National Institute of Chemical Physics and Biophysics, Tallinn, Estonia
S. Bhowmik, A. Carvalho Antunes De Oliveira, R.K. Dewanjee, K. Ehataht, M. Kadastik, M. Raidal, C. Veelken

Department of Physics, University of Helsinki, Helsinki, Finland
P. Eerola, H. Kirschenmann, J. Pekkanen, M. Voutilainen

Helsinki Institute of Physics, Helsinki, Finland
J. Havukainen, J.K. Heikkilä, T. Järvinen, V. Karimäki, R. Kinnunen, T. Lampén, K. Lassila-Perini, S. Laurila, S. Lehti, T. Lindén, P. Luukka, T. Mäenpää, H. Siikonen, E. Tuominen, J. Tuominiemi

Lappeenranta University of Technology, Lappeenranta, Finland
T. Tuuva

IRFU, CEA, Université Paris-Saclay, Gif-sur-Yvette, France
M. Besancon, F. Couderc, M. Dejardin, D. Denegri, J.L. Faure, F. Ferri, S. Ganjour, A. Givernaud, P. Gras, G. Hamel de Monchenault, P. Jarry, C. Leloup, E. Locci, J. Malcles, G. Negro, J. Rander, A. Rosowsky, M.Ö. Sahin, M. Titov

Laboratoire Leprince-Ringuet, Ecole polytechnique, CNRS/IN2P3, Université Paris-Saclay, Palaiseau, France
A. Abdulsalam[12], C. Amendola, I. Antropov, F. Beaudette, P. Busson, C. Charlot, R. Granier de Cassagnac, I. Kucher, A. Lobanov, J. Martin Blanco, M. Nguyen, C. Ochando, G. Ortona, P. Paganini, P. Pigard, R. Salerno, J.B. Sauvan, Y. Sirois, A.G. Stahl Leiton, A. Zabi, A. Zghiche

Université de Strasbourg, CNRS, IPHC UMR 7178, Strasbourg, France
J.-L. Agram[13], J. Andrea, D. Bloch, J.-M. Brom, E.C. Chabert, V. Cherepanov, C. Collard, E. Conte[13], J.-C. Fontaine[13], D. Gelé, U. Goerlach, M. Jansová, A.-C. Le Bihan, N. Tonon, P. Van Hove

Centre de Calcul de l'Institut National de Physique Nucleaire et de Physique des Particules, CNRS/IN2P3, Villeurbanne, France
S. Gadrat

Université de Lyon, Université Claude Bernard Lyon 1, CNRS-IN2P3, Institut de Physique Nucléaire de Lyon, Villeurbanne, France
S. Beauceron, C. Bernet, G. Boudoul, N. Chanon, R. Chierici, D. Contardo, P. Depasse, H. El Mamouni, J. Fay, L. Finco, S. Gascon, M. Gouzevitch, G. Grenier, B. Ille, F. Lagarde, I.B. Laktineh, H. Lattaud, M. Lethuillier, L. Mirabito, A.L. Pequegnot, S. Perries, A. Popov[14], V. Sordini, M. Vander Donckt, S. Viret, S. Zhang

Georgian Technical University, Tbilisi, Georgia
A. Khvedelidze[8]

Tbilisi State University, Tbilisi, Georgia
Z. Tsamalaidze[8]

RWTH Aachen University, I. Physikalisches Institut, Aachen, Germany
C. Autermann, L. Feld, M.K. Kiesel, K. Klein, M. Lipinski, M. Preuten, M.P. Rauch, C. Schomakers, J. Schulz, M. Teroerde, B. Wittmer, V. Zhukov[14]

RWTH Aachen University, III. Physikalisches Institut A, Aachen, Germany
A. Albert, D. Duchardt, M. Endres, M. Erdmann, T. Esch, R. Fischer, S. Ghosh, A. Güth, T. Hebbeker, C. Heidemann, K. Hoepfner, H. Keller, S. Knutzen, L. Mastrolorenzo, M. Merschmeyer, A. Meyer, P. Millet, S. Mukherjee, T. Pook, M. Radziej, H. Reithler, M. Rieger, F. Scheuch, A. Schmidt, D. Teyssier

RWTH Aachen University, III. Physikalisches Institut B, Aachen, Germany
G. Flügge, O. Hlushchenko, T. Kress, A. Künsken, T. Müller, A. Nehrkorn, A. Nowack, C. Pistone, O. Pooth, D. Roy, H. Sert, A. Stahl[15]

Deutsches Elektronen-Synchrotron, Hamburg, Germany
M. Aldaya Martin, T. Arndt, C. Asawatangtrakuldee, I. Babounikau, K. Beernaert, O. Behnke, U. Behrens, A. Bermúdez Martínez, D. Bertsche, A.A. Bin Anuar, K. Borras[16], V. Botta, A. Campbell, P. Connor, C. Contreras-Campana, F. Costanza, V. Danilov, A. De Wit, M.M. Defranchis, C. Diez Pardos, D. Domínguez Damiani, G. Eckerlin, T. Eichhorn, A. Elwood, E. Eren, E. Gallo[17], A. Geiser, J.M. Grados Luyando, A. Grohsjean, P. Gunnellini, M. Guthoff, M. Haranko, A. Harb, J. Hauk, H. Jung, M. Kasemann, J. Keaveney, C. Kleinwort, J. Knolle, D. Krücker, W. Lange, A. Lelek, T. Lenz, K. Lipka, W. Lohmann[18], R. Mankel, I.-A. Melzer-Pellmann, A.B. Meyer, M. Meyer, M. Missiroli, G. Mittag, J. Mnich, V. Myronenko, S.K. Pflitsch, D. Pitzl, A. Raspereza, M. Savitskyi, P. Saxena, P. Schütze, C. Schwanenberger, R. Shevchenko, A. Singh, H. Tholen, O. Turkot, A. Vagnerini, G.P. Van Onsem, R. Walsh, Y. Wen, K. Wichmann, C. Wissing, O. Zenaiev

University of Hamburg, Hamburg, Germany
R. Aggleton, S. Bein, L. Benato, A. Benecke, V. Blobel, M. Centis Vignali, T. Dreyer, E. Garutti, D. Gonzalez, J. Haller, A. Hinzmann, A. Karavdina, G. Kasieczka, R. Klanner, R. Kogler, N. Kovalchuk, S. Kurz, V. Kutzner, J. Lange, D. Marconi, J. Multhaup, M. Niedziela, D. Nowatschin, A. Perieanu, A. Reimers, O. Rieger, C. Scharf, P. Schleper, S. Schumann, J. Schwandt, J. Sonneveld, H. Stadie, G. Steinbrück, F.M. Stober, M. Stöver, D. Troendle, A. Vanhoefer, B. Vormwald

Karlsruher Institut fuer Technologie, Karlsruhe, Germany
M. Akbiyik, C. Barth, M. Baselga, S. Baur, E. Butz, R. Caspart, T. Chwalek, F. Colombo, W. De Boer, A. Dierlamm, K. El Morabit, N. Faltermann, B. Freund, M. Giffels, M.A. Harrendorf, F. Hartmann[15], S.M. Heindl, U. Husemann, F. Kassel[15], I. Katkov[14], S. Kudella, H. Mildner, S. Mitra, M.U. Mozer, Th. Müller, M. Plagge, G. Quast, K. Rabbertz, M. Schröder, I. Shvetsov, G. Sieber, H.J. Simonis, R. Ulrich, S. Wayand, M. Weber, T. Weiler, S. Williamson, C. Wöhrmann, R. Wolf

Institute of Nuclear and Particle Physics (INPP), NCSR Demokritos, Aghia Paraskevi, Greece
G. Anagnostou, G. Daskalakis, T. Geralis, A. Kyriakis, D. Loukas, G. Paspalaki, I. Topsis-Giotis

National and Kapodistrian University of Athens, Athens, Greece
G. Karathanasis, S. Kesisoglou, P. Kontaxakis, A. Panagiotou, I. Papavergou, N. Saoulidou, E. Tziaferi, K. Vellidis

National Technical University of Athens, Athens, Greece
K. Kousouris, I. Papakrivopoulos, G. Tsipolitis

University of Ioánnina, Ioánnina, Greece
I. Evangelou, C. Foudas, P. Gianneios, P. Katsoulis, P. Kokkas, S. Mallios, N. Manthos, I. Papadopoulos, E. Paradas, J. Strologas, F.A. Triantis, D. Tsitsonis

MTA-ELTE Lendület CMS Particle and Nuclear Physics Group, Eötvös Loránd University, Budapest, Hungary
M. Bartók[19], M. Csanad, N. Filipovic, P. Major, M.I. Nagy, G. Pasztor, O. Surányi, G.I. Veres

Wigner Research Centre for Physics, Budapest, Hungary

G. Bencze, C. Hajdu, D. Horvath[20], Á. Hunyadi, F. Sikler, T.Á. Vámi, V. Veszpremi, G. Vesztergombi[†]

Institute of Nuclear Research ATOMKI, Debrecen, Hungary
N. Beni, S. Czellar, J. Karancsi[21], A. Makovec, J. Molnar, Z. Szillasi

Institute of Physics, University of Debrecen, Debrecen, Hungary
P. Raics, Z.L. Trocsanyi, B. Ujvari

Indian Institute of Science (IISc), Bangalore, India
S. Choudhury, J.R. Komaragiri, P.C. Tiwari

National Institute of Science Education and Research, HBNI, Bhubaneswar, India
S. Bahinipati[22], C. Kar, P. Mal, K. Mandal, A. Nayak[23], D.K. Sahoo[22], S.K. Swain

Panjab University, Chandigarh, India
S. Bansal, S.B. Beri, V. Bhatnagar, S. Chauhan, R. Chawla, N. Dhingra, R. Gupta, A. Kaur, A. Kaur, M. Kaur, S. Kaur, R. Kumar, P. Kumari, M. Lohan, A. Mehta, K. Sandeep, S. Sharma, J.B. Singh, G. Walia

University of Delhi, Delhi, India
A. Bhardwaj, B.C. Choudhary, R.B. Garg, M. Gola, S. Keshri, Ashok Kumar, S. Malhotra, M. Naimuddin, P. Priyanka, K. Ranjan, Aashaq Shah, R. Sharma

Saha Institute of Nuclear Physics, HBNI, Kolkata, India
R. Bhardwaj[24], M. Bharti, R. Bhattacharya, S. Bhattacharya, U. Bhawandeep[24], D. Bhowmik, S. Dey, S. Dutt[24], S. Dutta, S. Ghosh, K. Mondal, S. Nandan, A. Purohit, P.K. Rout, A. Roy, S. Roy Chowdhury, G. Saha, S. Sarkar, M. Sharan, B. Singh, S. Thakur[24]

Indian Institute of Technology Madras, Madras, India
P.K. Behera

Bhabha Atomic Research Centre, Mumbai, India
R. Chudasama, D. Dutta, V. Jha, V. Kumar, P.K. Netrakanti, L.M. Pant, P. Shukla

Tata Institute of Fundamental Research-A, Mumbai, India
T. Aziz, M.A. Bhat, S. Dugad, G.B. Mohanty, N. Sur, B. Sutar, RavindraKumar Verma

Tata Institute of Fundamental Research-B, Mumbai, India
S. Banerjee, S. Bhattacharya, S. Chatterjee, P. Das, M. Guchait, Sa. Jain, S. Karmakar, S. Kumar, M. Maity[25], G. Majumder, K. Mazumdar, N. Sahoo, T. Sarkar[25]

Indian Institute of Science Education and Research (IISER), Pune, India
S. Chauhan, S. Dube, V. Hegde, A. Kapoor, K. Kothekar, S. Pandey, A. Rane, S. Sharma

Institute for Research in Fundamental Sciences (IPM), Tehran, Iran
S. Chenarani[26], E. Eskandari Tadavani, S.M. Etesami[26], M. Khakzad, M. Mohammadi Najafabadi, M. Naseri, F. Rezaei Hosseinabadi, B. Safarzadeh[27], M. Zeinali

University College Dublin, Dublin, Ireland
M. Felcini, M. Grunewald

INFN Sezione di Bari [a], Università di Bari [b], Politecnico di Bari [c], Bari, Italy
M. Abbrescia[a,b], C. Calabria[a,b], A. Colaleo[a], D. Creanza[a,c], L. Cristella[a,b], N. De Filippis[a,c], M. De Palma[a,b], A. Di Florio[a,b], F. Errico[a,b], L. Fiore[a], A. Gelmi[a,b], G. Iaselli[a,c], M. Ince[a,b], S. Lezki[a,b], G. Maggi[a,c], M. Maggi[a], G. Miniello[a,b], S. My[a,b], S. Nuzzo[a,b], A. Pompili[a,b],

G. Pugliese[a,c], R. Radogna[a], A. Ranieri[a], G. Selvaggi[a,b], A. Sharma[a], L. Silvestris[a], R. Venditti[a], P. Verwilligen[a], G. Zito[a]

INFN Sezione di Bologna [a], Università di Bologna [b], Bologna, Italy
G. Abbiendi[a], C. Battilana[a,b], D. Bonacorsi[a,b], L. Borgonovi[a,b], S. Braibant-Giacomelli[a,b], R. Campanini[a,b], P. Capiluppi[a,b], A. Castro[a,b], F.R. Cavallo[a], S.S. Chhibra[a,b], C. Ciocca[a], G. Codispoti[a,b], M. Cuffiani[a,b], G.M. Dallavalle[a], F. Fabbri[a], A. Fanfani[a,b], P. Giacomelli[a], C. Grandi[a], L. Guiducci[a,b], F. Iemmi[a,b], S. Marcellini[a], G. Masetti[a], A. Montanari[a], F.L. Navarria[a,b], A. Perrotta[a], F. Primavera[a,b,15], A.M. Rossi[a,b], T. Rovelli[a,b], G.P. Siroli[a,b], N. Tosi[a]

INFN Sezione di Catania [a], Università di Catania [b], Catania, Italy
S. Albergo[a,b], A. Di Mattia[a], R. Potenza[a,b], A. Tricomi[a,b], C. Tuve[a,b]

INFN Sezione di Firenze [a], Università di Firenze [b], Firenze, Italy
G. Barbagli[a], K. Chatterjee[a,b], V. Ciulli[a,b], C. Civinini[a], R. D'Alessandro[a,b], E. Focardi[a,b], G. Latino, P. Lenzi[a,b], M. Meschini[a], S. Paoletti[a], L. Russo[a,28], G. Sguazzoni[a], D. Strom[a], L. Viliani[a]

INFN Laboratori Nazionali di Frascati, Frascati, Italy
L. Benussi, S. Bianco, F. Fabbri, D. Piccolo

INFN Sezione di Genova [a], Università di Genova [b], Genova, Italy
F. Ferro[a], F. Ravera[a,b], E. Robutti[a], S. Tosi[a,b]

INFN Sezione di Milano-Bicocca [a], Università di Milano-Bicocca [b], Milano, Italy
A. Benaglia[a], A. Beschi[b], L. Brianza[a,b], F. Brivio[a,b], V. Ciriolo[a,b,15], S. Di Guida[a,d,15], M.E. Dinardo[a,b], S. Fiorendi[a,b], S. Gennai[a], A. Ghezzi[a,b], P. Govoni[a,b], M. Malberti[a,b], S. Malvezzi[a], A. Massironi[a,b], D. Menasce[a], L. Moroni[a], M. Paganoni[a,b], D. Pedrini[a], S. Ragazzi[a,b], T. Tabarelli de Fatis[a,b], D. Zuolo

INFN Sezione di Napoli [a], Università di Napoli 'Federico II' [b], Napoli, Italy, Università della Basilicata [c], Potenza, Italy, Università G. Marconi [d], Roma, Italy
S. Buontempo[a], N. Cavallo[a,c], A. Di Crescenzo[a,b], F. Fabozzi[a,c], F. Fienga[a], G. Galati[a], A.O.M. Iorio[a,b], W.A. Khan[a], L. Lista[a], S. Meola[a,d,15], P. Paolucci[a,15], C. Sciacca[a,b], E. Voevodina[a,b]

INFN Sezione di Padova [a], Università di Padova [b], Padova, Italy, Università di Trento [c], Trento, Italy
P. Azzi[a], N. Bacchetta[a], D. Bisello[a,b], A. Boletti[a,b], A. Bragagnolo, R. Carlin[a,b], P. Checchia[a], M. Dall'Osso[a,b], P. De Castro Manzano[a], T. Dorigo[a], U. Dosselli[a], F. Gasparini[a,b], U. Gasparini[a,b], A. Gozzelino[a], S.Y. Hoh, S. Lacaprara[a], P. Lujan, M. Margoni[a,b], A.T. Meneguzzo[a,b], J. Pazzini[a,b], P. Ronchese[a,b], R. Rossin[a,b], F. Simonetto[a,b], A. Tiko, E. Torassa[a], M. Zanetti[a,b], P. Zotto[a,b], G. Zumerle[a,b]

INFN Sezione di Pavia [a], Università di Pavia [b], Pavia, Italy
A. Braghieri[a], A. Magnani[a], P. Montagna[a,b], S.P. Ratti[a,b], V. Re[a], M. Ressegotti[a,b], C. Riccardi[a,b], P. Salvini[a], I. Vai[a,b], P. Vitulo[a,b]

INFN Sezione di Perugia [a], Università di Perugia [b], Perugia, Italy
L. Alunni Solestizi[a,b], M. Biasini[a,b], G.M. Bilei[a], C. Cecchi[a,b], D. Ciangottini[a,b], L. Fanò[a,b], P. Lariccia[a,b], R. Leonardi[a,b], E. Manoni[a], G. Mantovani[a,b], V. Mariani[a,b], M. Menichelli[a], A. Rossi[a,b], A. Santocchia[a,b], D. Spiga[a]

INFN Sezione di Pisa [a]**, Università di Pisa** [b]**, Scuola Normale Superiore di Pisa** [c]**, Pisa, Italy**
K. Androsov[a], P. Azzurri[a], G. Bagliesi[a], L. Bianchini[a], T. Boccali[a], L. Borrello, R. Castaldi[a], M.A. Ciocci[a,b], R. Dell'Orso[a], G. Fedi[a], F. Fiori[a,c], L. Giannini[a,c], A. Giassi[a], M.T. Grippo[a], F. Ligabue[a,c], E. Manca[a,c], G. Mandorli[a,c], A. Messineo[a,b], F. Palla[a], A. Rizzi[a,b], P. Spagnolo[a], R. Tenchini[a], G. Tonelli[a,b], A. Venturi[a], P.G. Verdini[a]

INFN Sezione di Roma [a]**, Sapienza Università di Roma** [b]**, Rome, Italy**
L. Barone[a,b], F. Cavallari[a], M. Cipriani[a,b], N. Daci[a], D. Del Re[a,b], E. Di Marco[a,b], M. Diemoz[a], S. Gelli[a,b], E. Longo[a,b], B. Marzocchi[a,b], P. Meridiani[a], G. Organtini[a,b], F. Pandolfi[a], R. Paramatti[a,b], F. Preiato[a,b], S. Rahatlou[a,b], C. Rovelli[a], F. Santanastasio[a,b]

INFN Sezione di Torino [a]**, Università di Torino** [b]**, Torino, Italy, Università del Piemonte Orientale** [c]**, Novara, Italy**
N. Amapane[a,b], R. Arcidiacono[a,c], S. Argiro[a,b], M. Arneodo[a,c], N. Bartosik[a], R. Bellan[a,b], C. Biino[a], N. Cartiglia[a], F. Cenna[a,b], S. Cometti, M. Costa[a,b], R. Covarelli[a,b], N. Demaria[a], B. Kiani[a,b], C. Mariotti[a], S. Maselli[a], E. Migliore[a,b], V. Monaco[a,b], E. Monteil[a,b], M. Monteno[a], M.M. Obertino[a,b], L. Pacher[a,b], N. Pastrone[a], M. Pelliccioni[a], G.L. Pinna Angioni[a,b], A. Romero[a,b], M. Ruspa[a,c], R. Sacchi[a,b], K. Shchelina[a,b], V. Sola[a], A. Solano[a,b], D. Soldi, A. Staiano[a]

INFN Sezione di Trieste [a]**, Università di Trieste** [b]**, Trieste, Italy**
S. Belforte[a], V. Candelise[a,b], M. Casarsa[a], F. Cossutti[a], G. Della Ricca[a,b], F. Vazzoler[a,b], A. Zanetti[a]

Kyungpook National University, Daegu, Korea
D.H. Kim, G.N. Kim, M.S. Kim, J. Lee, S. Lee, S.W. Lee, C.S. Moon, Y.D. Oh, S. Sekmen, D.C. Son, Y.C. Yang

Chonnam National University, Institute for Universe and Elementary Particles, Kwangju, Korea
H. Kim, D.H. Moon, G. Oh

Hanyang University, Seoul, Korea
J. Goh[29], T.J. Kim

Korea University, Seoul, Korea
S. Cho, S. Choi, Y. Go, D. Gyun, S. Ha, B. Hong, Y. Jo, K. Lee, K.S. Lee, S. Lee, J. Lim, S.K. Park, Y. Roh

Sejong University, Seoul, Korea
H.S. Kim

Seoul National University, Seoul, Korea
J. Almond, J. Kim, J.S. Kim, H. Lee, K. Lee, K. Nam, S.B. Oh, B.C. Radburn-Smith, S.h. Seo, U.K. Yang, H.D. Yoo, G.B. Yu

University of Seoul, Seoul, Korea
D. Jeon, H. Kim, J.H. Kim, J.S.H. Lee, I.C. Park

Sungkyunkwan University, Suwon, Korea
Y. Choi, C. Hwang, J. Lee, I. Yu

Vilnius University, Vilnius, Lithuania
V. Dudenas, A. Juodagalvis, J. Vaitkus

National Centre for Particle Physics, Universiti Malaya, Kuala Lumpur, Malaysia
I. Ahmed, Z.A. Ibrahim, M.A.B. Md Ali[30], F. Mohamad Idris[31], W.A.T. Wan Abdullah,
M.N. Yusli, Z. Zolkapli

Universidad de Sonora (UNISON), Hermosillo, Mexico
A. Castaneda Hernandez, J.A. Murillo Quijada

Centro de Investigacion y de Estudios Avanzados del IPN, Mexico City, Mexico
H. Castilla-Valdez, E. De La Cruz-Burelo, M.C. Duran-Osuna, I. Heredia-De La Cruz[32],
R. Lopez-Fernandez, J. Mejia Guisao, R.I. Rabadan-Trejo, M. Ramirez-Garcia, G. Ramirez-
Sanchez, R Reyes-Almanza, A. Sanchez-Hernandez

Universidad Iberoamericana, Mexico City, Mexico
S. Carrillo Moreno, C. Oropeza Barrera, F. Vazquez Valencia

Benemerita Universidad Autonoma de Puebla, Puebla, Mexico
J. Eysermans, I. Pedraza, H.A. Salazar Ibarguen, C. Uribe Estrada

Universidad Autónoma de San Luis Potosí, San Luis Potosí, Mexico
A. Morelos Pineda

University of Auckland, Auckland, New Zealand
D. Krofcheck

University of Canterbury, Christchurch, New Zealand
S. Bheesette, P.H. Butler

National Centre for Physics, Quaid-I-Azam University, Islamabad, Pakistan
A. Ahmad, M. Ahmad, M.I. Asghar, Q. Hassan, H.R. Hoorani, A. Saddique, M.A. Shah,
M. Shoaib, M. Waqas

National Centre for Nuclear Research, Swierk, Poland
H. Bialkowska, M. Bluj, B. Boimska, T. Frueboes, M. Górski, M. Kazana, K. Nawrocki,
M. Szleper, P. Traczyk, P. Zalewski

Institute of Experimental Physics, Faculty of Physics, University of Warsaw, Warsaw, Poland
K. Bunkowski, A. Byszuk[33], K. Doroba, A. Kalinowski, M. Konecki, J. Krolikowski, M. Misiura,
M. Olszewski, A. Pyskir, M. Walczak

Laboratório de Instrumentação e Física Experimental de Partículas, Lisboa, Portugal
M. Araujo, P. Bargassa, C. Beirão Da Cruz E Silva, A. Di Francesco, P. Faccioli, B. Galinhas,
M. Gallinaro, J. Hollar, N. Leonardo, L. Lloret Iglesias, M.V. Nemallapudi, J. Seixas, G. Strong,
O. Toldaiev, D. Vadruccio, J. Varela

Joint Institute for Nuclear Research, Dubna, Russia
S. Afanasiev, V. Alexakhin, P. Bunin, M. Gavrilenko, A. Golunov, I. Golutvin, N. Gorbounov,
V. Karjavin, A. Lanev, A. Malakhov, V. Matveev[34,35], P. Moisenz, V. Palichik, V. Perelygin,
M. Savina, S. Shmatov, V. Smirnov, N. Voytishin, A. Zarubin

Petersburg Nuclear Physics Institute, Gatchina (St. Petersburg), Russia
V. Golovtsov, Y. Ivanov, V. Kim[36], E. Kuznetsova[37], P. Levchenko, V. Murzin, V. Oreshkin,
I. Smirnov, D. Sosnov, V. Sulimov, L. Uvarov, S. Vavilov, A. Vorobyev

Institute for Nuclear Research, Moscow, Russia
Yu. Andreev, A. Dermenev, S. Gninenko, N. Golubev, A. Karneyeu, M. Kirsanov, N. Krasnikov,
A. Pashenkov, D. Tlisov, A. Toropin

Institute for Theoretical and Experimental Physics, Moscow, Russia
V. Epshteyn, V. Gavrilov, N. Lychkovskaya, V. Popov, I. Pozdnyakov, G. Safronov, A. Spiridonov, A. Stepennov, V. Stolin, M. Toms, E. Vlasov, A. Zhokin

Moscow Institute of Physics and Technology, Moscow, Russia
T. Aushev

National Research Nuclear University 'Moscow Engineering Physics Institute' (MEPhI), Moscow, Russia
R. Chistov[38], M. Danilov[38], P. Parygin, D. Philippov, S. Polikarpov[38], E. Tarkovskii

P.N. Lebedev Physical Institute, Moscow, Russia
V. Andreev, M. Azarkin[35], I. Dremin[35], M. Kirakosyan[35], S.V. Rusakov, A. Terkulov

Skobeltsyn Institute of Nuclear Physics, Lomonosov Moscow State University, Moscow, Russia
A. Baskakov, A. Belyaev, E. Boos, V. Bunichev, M. Dubinin[39], L. Dudko, A. Ershov, V. Klyukhin, O. Kodolova, N. Korneeva, I. Lokhtin, I. Miagkov, S. Obraztsov, M. Perfilov, V. Savrin

Novosibirsk State University (NSU), Novosibirsk, Russia
V. Blinov[40], T. Dimova[40], L. Kardapoltsev[40], D. Shtol[40], Y. Skovpen[40]

Institute for High Energy Physics of National Research Centre 'Kurchatov Institute', Protvino, Russia
I. Azhgirey, I. Bayshev, S. Bitioukov, D. Elumakhov, A. Godizov, V. Kachanov, A. Kalinin, D. Konstantinov, P. Mandrik, V. Petrov, R. Ryutin, S. Slabospitskii, A. Sobol, S. Troshin, N. Tyurin, A. Uzunian, A. Volkov

National Research Tomsk Polytechnic University, Tomsk, Russia
A. Babaev, S. Baidali, V. Okhotnikov

University of Belgrade, Faculty of Physics and Vinca Institute of Nuclear Sciences, Belgrade, Serbia
P. Adzic[41], P. Cirkovic, D. Devetak, M. Dordevic, J. Milosevic

Centro de Investigaciones Energéticas Medioambientales y Tecnológicas (CIEMAT), Madrid, Spain
J. Alcaraz Maestre, A. Álvarez Fernández, I. Bachiller, M. Barrio Luna, J.A. Brochero Cifuentes, M. Cerrada, N. Colino, B. De La Cruz, A. Delgado Peris, C. Fernandez Bedoya, J.P. Fernández Ramos, J. Flix, M.C. Fouz, O. Gonzalez Lopez, S. Goy Lopez, J.M. Hernandez, M.I. Josa, D. Moran, A. Pérez-Calero Yzquierdo, J. Puerta Pelayo, I. Redondo, L. Romero, M.S. Soares, A. Triossi

Universidad Autónoma de Madrid, Madrid, Spain
C. Albajar, J.F. de Trocóniz

Universidad de Oviedo, Oviedo, Spain
J. Cuevas, C. Erice, J. Fernandez Menendez, S. Folgueras, I. Gonzalez Caballero, J.R. González Fernández, E. Palencia Cortezon, V. Rodríguez Bouza, S. Sanchez Cruz, P. Vischia, J.M. Vizan Garcia

Instituto de Física de Cantabria (IFCA), CSIC-Universidad de Cantabria, Santander, Spain
I.J. Cabrillo, A. Calderon, B. Chazin Quero, J. Duarte Campderros, M. Fernandez, P.J. Fernández Manteca, A. García Alonso, J. Garcia-Ferrero, G. Gomez, A. Lopez Virto,

J. Marco, C. Martinez Rivero, P. Martinez Ruiz del Arbol, F. Matorras, J. Piedra Gomez, C. Prieels, T. Rodrigo, A. Ruiz-Jimeno, L. Scodellaro, N. Trevisani, I. Vila, R. Vilar Cortabitarte

CERN, European Organization for Nuclear Research, Geneva, Switzerland
D. Abbaneo, B. Akgun, E. Auffray, P. Baillon, A.H. Ball, D. Barney, J. Bendavid, M. Bianco, A. Bocci, C. Botta, E. Brondolin, T. Camporesi, M. Cepeda, G. Cerminara, E. Chapon, Y. Chen, G. Cucciati, D. d'Enterria, A. Dabrowski, V. Daponte, A. David, A. De Roeck, N. Deelen, M. Dobson, M. Dünser, N. Dupont, A. Elliott-Peisert, P. Everaerts, F. Fallavollita[42], D. Fasanella, G. Franzoni, J. Fulcher, W. Funk, D. Gigi, A. Gilbert, K. Gill, F. Glege, M. Guilbaud, D. Gulhan, J. Hegeman, V. Innocente, A. Jafari, P. Janot, O. Karacheban[18], J. Kieseler, A. Kornmayer, M. Krammer[1], C. Lange, P. Lecoq, C. Lourenço, L. Malgeri, M. Mannelli, F. Meijers, J.A. Merlin, S. Mersi, E. Meschi, P. Milenovic[43], F. Moortgat, M. Mulders, J. Ngadiuba, S. Orfanelli, L. Orsini, F. Pantaleo[15], L. Pape, E. Perez, M. Peruzzi, A. Petrilli, G. Petrucciani, A. Pfeiffer, M. Pierini, F.M. Pitters, D. Rabady, A. Racz, T. Reis, G. Rolandi[44], M. Rovere, H. Sakulin, C. Schäfer, C. Schwick, M. Seidel, M. Selvaggi, A. Sharma, P. Silva, P. Sphicas[45], A. Stakia, J. Steggemann, M. Tosi, D. Treille, A. Tsirou, V. Veckalns[46], W.D. Zeuner

Paul Scherrer Institut, Villigen, Switzerland
L. Caminada[47], K. Deiters, W. Erdmann, R. Horisberger, Q. Ingram, H.C. Kaestli, D. Kotlinski, U. Langenegger, T. Rohe, S.A. Wiederkehr

ETH Zurich - Institute for Particle Physics and Astrophysics (IPA), Zurich, Switzerland
M. Backhaus, L. Bäni, P. Berger, N. Chernyavskaya, G. Dissertori, M. Dittmar, M. Donegà, C. Dorfer, C. Grab, C. Heidegger, D. Hits, J. Hoss, T. Klijnsma, W. Lustermann, R.A. Manzoni, M. Marionneau, M.T. Meinhard, F. Micheli, P. Musella, F. Nessi-Tedaldi, J. Pata, F. Pauss, G. Perrin, L. Perrozzi, S. Pigazzini, M. Quittnat, D. Ruini, D.A. Sanz Becerra, M. Schönenberger, L. Shchutska, V.R. Tavolaro, K. Theofilatos, M.L. Vesterbacka Olsson, R. Wallny, D.H. Zhu

Universität Zürich, Zurich, Switzerland
T.K. Aarrestad, C. Amsler[48], D. Brzhechko, M.F. Canelli, A. De Cosa, R. Del Burgo, S. Donato, C. Galloni, T. Hreus, B. Kilminster, I. Neutelings, D. Pinna, G. Rauco, P. Robmann, D. Salerno, K. Schweiger, C. Seitz, Y. Takahashi, A. Zucchetta

National Central University, Chung-Li, Taiwan
Y.H. Chang, K.y. Cheng, T.H. Doan, Sh. Jain, R. Khurana, C.M. Kuo, W. Lin, A. Pozdnyakov, S.S. Yu

National Taiwan University (NTU), Taipei, Taiwan
P. Chang, Y. Chao, K.F. Chen, P.H. Chen, W.-S. Hou, Arun Kumar, Y.y. Li, Y.F. Liu, R.-S. Lu, E. Paganis, A. Psallidas, A. Steen

Chulalongkorn University, Faculty of Science, Department of Physics, Bangkok, Thailand
B. Asavapibhop, N. Srimanobhas, N. Suwonjandee

Çukurova University, Physics Department, Science and Art Faculty, Adana, Turkey
A. Bat, F. Boran, S. Damarseckin, Z.S. Demiroglu, F. Dolek, C. Dozen, I. Dumanoglu, S. Girgis, G. Gokbulut, Y. Guler, E. Gurpinar, I. Hos[49], C. Isik, E.E. Kangal[50], O. Kara, A. Kayis Topaksu, U. Kiminsu, M. Oglakci, G. Onengut, K. Ozdemir[51], S. Ozturk[52], D. Sunar Cerci[53], B. Tali[53], U.G. Tok, H. Topakli[52], S. Turkcapar, I.S. Zorbakir, C. Zorbilmez

Middle East Technical University, Physics Department, Ankara, Turkey
B. Isildak[54], G. Karapinar[55], M. Yalvac, M. Zeyrek

Bogazici University, Istanbul, Turkey
I.O. Atakisi, E. Gülmez, M. Kaya[56], O. Kaya[57], S. Ozkorucuklu[58], S. Tekten, E.A. Yetkin[59]

Istanbul Technical University, Istanbul, Turkey
M.N. Agaras, S. Atay, A. Cakir, K. Cankocak, Y. Komurcu, S. Sen[60]

Institute for Scintillation Materials of National Academy of Science of Ukraine, Kharkov, Ukraine
B. Grynyov

National Scientific Center, Kharkov Institute of Physics and Technology, Kharkov, Ukraine
L. Levchuk

University of Bristol, Bristol, United Kingdom
F. Ball, L. Beck, J.J. Brooke, D. Burns, E. Clement, D. Cussans, O. Davignon, H. Flacher, J. Goldstein, G.P. Heath, H.F. Heath, L. Kreczko, D.M. Newbold[61], S. Paramesvaran, B. Penning, T. Sakuma, D. Smith, V.J. Smith, J. Taylor, A. Titterton

Rutherford Appleton Laboratory, Didcot, United Kingdom
K.W. Bell, A. Belyaev[62], C. Brew, R.M. Brown, D. Cieri, D.J.A. Cockerill, J.A. Coughlan, K. Harder, S. Harper, J. Linacre, E. Olaiya, D. Petyt, C.H. Shepherd-Themistocleous, A. Thea, I.R. Tomalin, T. Williams, W.J. Womersley

Imperial College, London, United Kingdom
G. Auzinger, R. Bainbridge, P. Bloch, J. Borg, S. Breeze, O. Buchmuller, A. Bundock, S. Casasso, D. Colling, L. Corpe, P. Dauncey, G. Davies, M. Della Negra, R. Di Maria, Y. Haddad, G. Hall, G. Iles, T. James, M. Komm, C. Laner, L. Lyons, A.-M. Magnan, S. Malik, A. Martelli, J. Nash[63], A. Nikitenko[7], V. Palladino, M. Pesaresi, A. Richards, A. Rose, E. Scott, C. Seez, A. Shtipliyski, G. Singh, M. Stoye, T. Strebler, S. Summers, A. Tapper, K. Uchida, T. Virdee[15], N. Wardle, D. Winterbottom, J. Wright, S.C. Zenz

Brunel University, Uxbridge, United Kingdom
J.E. Cole, P.R. Hobson, A. Khan, P. Kyberd, C.K. Mackay, A. Morton, I.D. Reid, L. Teodorescu, S. Zahid

Baylor University, Waco, USA
K. Call, J. Dittmann, K. Hatakeyama, H. Liu, C. Madrid, B. Mcmaster, N. Pastika, C. Smith

Catholic University of America, Washington DC, USA
R. Bartek, A. Dominguez

The University of Alabama, Tuscaloosa, USA
A. Buccilli, S.I. Cooper, C. Henderson, P. Rumerio, C. West

Boston University, Boston, USA
D. Arcaro, T. Bose, D. Gastler, D. Rankin, C. Richardson, J. Rohlf, L. Sulak, D. Zou

Brown University, Providence, USA
G. Benelli, X. Coubez, D. Cutts, M. Hadley, J. Hakala, U. Heintz, J.M. Hogan[64], K.H.M. Kwok, E. Laird, G. Landsberg, J. Lee, Z. Mao, M. Narain, S. Piperov, S. Sagir[65], R. Syarif, E. Usai, D. Yu

University of California, Davis, Davis, USA
R. Band, C. Brainerd, R. Breedon, D. Burns, M. Calderon De La Barca Sanchez, M. Chertok, J. Conway, R. Conway, P.T. Cox, R. Erbacher, C. Flores, G. Funk, W. Ko, O. Kukral, R. Lander, C. Mclean, M. Mulhearn, D. Pellett, J. Pilot, S. Shalhout, M. Shi, D. Stolp, D. Taylor, K. Tos, M. Tripathi, Z. Wang, F. Zhang

University of California, Los Angeles, USA
M. Bachtis, C. Bravo, R. Cousins, A. Dasgupta, A. Florent, J. Hauser, M. Ignatenko, N. Mccoll, S. Regnard, D. Saltzberg, C. Schnaible, V. Valuev

University of California, Riverside, Riverside, USA
E. Bouvier, K. Burt, R. Clare, J.W. Gary, S.M.A. Ghiasi Shirazi, G. Hanson, G. Karapostoli, E. Kennedy, F. Lacroix, O.R. Long, M. Olmedo Negrete, M.I. Paneva, W. Si, L. Wang, H. Wei, S. Wimpenny, B.R. Yates

University of California, San Diego, La Jolla, USA
J.G. Branson, S. Cittolin, M. Derdzinski, R. Gerosa, D. Gilbert, B. Hashemi, A. Holzner, D. Klein, G. Kole, V. Krutelyov, J. Letts, M. Masciovecchio, D. Olivito, S. Padhi, M. Pieri, M. Sani, V. Sharma, S. Simon, M. Tadel, A. Vartak, S. Wasserbaech[66], J. Wood, F. Würthwein, A. Yagil, G. Zevi Della Porta

University of California, Santa Barbara - Department of Physics, Santa Barbara, USA
N. Amin, R. Bhandari, J. Bradmiller-Feld, C. Campagnari, M. Citron, A. Dishaw, V. Dutta, M. Franco Sevilla, L. Gouskos, R. Heller, J. Incandela, A. Ovcharova, H. Qu, J. Richman, D. Stuart, I. Suarez, S. Wang, J. Yoo

California Institute of Technology, Pasadena, USA
D. Anderson, A. Bornheim, J.M. Lawhorn, H.B. Newman, T.Q. Nguyen, M. Spiropulu, J.R. Vlimant, R. Wilkinson, S. Xie, Z. Zhang, R.Y. Zhu

Carnegie Mellon University, Pittsburgh, USA
M.B. Andrews, T. Ferguson, T. Mudholkar, M. Paulini, M. Sun, I. Vorobiev, M. Weinberg

University of Colorado Boulder, Boulder, USA
J.P. Cumalat, W.T. Ford, F. Jensen, A. Johnson, M. Krohn, S. Leontsinis, E. MacDonald, T. Mulholland, K. Stenson, K.A. Ulmer, S.R. Wagner

Cornell University, Ithaca, USA
J. Alexander, J. Chaves, Y. Cheng, J. Chu, A. Datta, K. Mcdermott, N. Mirman, J.R. Patterson, D. Quach, A. Rinkevicius, A. Ryd, L. Skinnari, L. Soffi, S.M. Tan, Z. Tao, J. Thom, J. Tucker, P. Wittich, M. Zientek

Fermi National Accelerator Laboratory, Batavia, USA
S. Abdullin, M. Albrow, M. Alyari, G. Apollinari, A. Apresyan, A. Apyan, S. Banerjee, L.A.T. Bauerdick, A. Beretvas, J. Berryhill, P.C. Bhat, G. Bolla[†], K. Burkett, J.N. Butler, A. Canepa, G.B. Cerati, H.W.K. Cheung, F. Chlebana, M. Cremonesi, J. Duarte, V.D. Elvira, J. Freeman, Z. Gecse, E. Gottschalk, L. Gray, D. Green, S. Grünendahl, O. Gutsche, J. Hanlon, R.M. Harris, S. Hasegawa, J. Hirschauer, Z. Hu, B. Jayatilaka, S. Jindariani, M. Johnson, U. Joshi, B. Klima, M.J. Kortelainen, B. Kreis, S. Lammel, D. Lincoln, R. Lipton, M. Liu, T. Liu, J. Lykken, K. Maeshima, J.M. Marraffino, D. Mason, P. McBride, P. Merkel, S. Mrenna, S. Nahn, V. O'Dell, K. Pedro, C. Pena, O. Prokofyev, G. Rakness, L. Ristori, A. Savoy-Navarro[67], B. Schneider, E. Sexton-Kennedy, A. Soha, W.J. Spalding, L. Spiegel, S. Stoynev, J. Strait, N. Strobbe, L. Taylor, S. Tkaczyk, N.V. Tran, L. Uplegger, E.W. Vaandering, C. Vernieri, M. Verzocchi, R. Vidal, M. Wang, H.A. Weber, A. Whitbeck

University of Florida, Gainesville, USA
D. Acosta, P. Avery, P. Bortignon, D. Bourilkov, A. Brinkerhoff, L. Cadamuro, A. Carnes, M. Carver, D. Curry, R.D. Field, S.V. Gleyzer, B.M. Joshi, J. Konigsberg, A. Korytov, P. Ma, K. Matchev, H. Mei, G. Mitselmakher, K. Shi, D. Sperka, J. Wang, S. Wang

Florida International University, Miami, USA
Y.R. Joshi, S. Linn

Florida State University, Tallahassee, USA
A. Ackert, T. Adams, A. Askew, S. Hagopian, V. Hagopian, K.F. Johnson, T. Kolberg, G. Martinez, T. Perry, H. Prosper, A. Saha, C. Schiber, V. Sharma, R. Yohay

Florida Institute of Technology, Melbourne, USA
M.M. Baarmand, V. Bhopatkar, S. Colafranceschi, M. Hohlmann, D. Noonan, M. Rahmani, T. Roy, F. Yumiceva

University of Illinois at Chicago (UIC), Chicago, USA
M.R. Adams, L. Apanasevich, D. Berry, R.R. Betts, R. Cavanaugh, X. Chen, S. Dittmer, O. Evdokimov, C.E. Gerber, D.A. Hangal, D.J. Hofman, K. Jung, J. Kamin, C. Mills, I.D. Sandoval Gonzalez, M.B. Tonjes, N. Varelas, H. Wang, X. Wang, Z. Wu, J. Zhang

The University of Iowa, Iowa City, USA
M. Alhusseini, B. Bilki[68], W. Clarida, K. Dilsiz[69], S. Durgut, R.P. Gandrajula, M. Haytmyradov, V. Khristenko, J.-P. Merlo, A. Mestvirishvili, A. Moeller, J. Nachtman, H. Ogul[70], Y. Onel, F. Ozok[71], A. Penzo, C. Snyder, E. Tiras, J. Wetzel

Johns Hopkins University, Baltimore, USA
B. Blumenfeld, A. Cocoros, N. Eminizer, D. Fehling, L. Feng, A.V. Gritsan, W.T. Hung, P. Maksimovic, J. Roskes, U. Sarica, M. Swartz, M. Xiao, C. You

The University of Kansas, Lawrence, USA
A. Al-bataineh, P. Baringer, A. Bean, S. Boren, J. Bowen, A. Bylinkin, J. Castle, S. Khalil, A. Kropivnitskaya, D. Majumder, W. Mcbrayer, M. Murray, C. Rogan, S. Sanders, E. Schmitz, J.D. Tapia Takaki, Q. Wang

Kansas State University, Manhattan, USA
S. Duric, A. Ivanov, K. Kaadze, D. Kim, Y. Maravin, D.R. Mendis, T. Mitchell, A. Modak, A. Mohammadi, L.K. Saini, N. Skhirtladze

Lawrence Livermore National Laboratory, Livermore, USA
F. Rebassoo, D. Wright

University of Maryland, College Park, USA
A. Baden, O. Baron, A. Belloni, S.C. Eno, Y. Feng, C. Ferraioli, N.J. Hadley, S. Jabeen, G.Y. Jeng, R.G. Kellogg, J. Kunkle, A.C. Mignerey, F. Ricci-Tam, Y.H. Shin, A. Skuja, S.C. Tonwar, K. Wong

Massachusetts Institute of Technology, Cambridge, USA
D. Abercrombie, B. Allen, V. Azzolini, A. Baty, G. Bauer, R. Bi, S. Brandt, W. Busza, I.A. Cali, M. D'Alfonso, Z. Demiragli, G. Gomez Ceballos, M. Goncharov, P. Harris, D. Hsu, M. Hu, Y. Iiyama, G.M. Innocenti, M. Klute, D. Kovalskyi, Y.-J. Lee, P.D. Luckey, B. Maier, A.C. Marini, C. Mcginn, C. Mironov, S. Narayanan, X. Niu, C. Paus, C. Roland, G. Roland, G.S.F. Stephans, K. Sumorok, K. Tatar, D. Velicanu, J. Wang, T.W. Wang, B. Wyslouch, S. Zhaozhong

University of Minnesota, Minneapolis, USA
A.C. Benvenuti, R.M. Chatterjee, A. Evans, P. Hansen, S. Kalafut, Y. Kubota, Z. Lesko, J. Mans, S. Nourbakhsh, N. Ruckstuhl, R. Rusack, J. Turkewitz, M.A. Wadud

University of Mississippi, Oxford, USA
J.G. Acosta, S. Oliveros

University of Nebraska-Lincoln, Lincoln, USA
E. Avdeeva, K. Bloom, D.R. Claes, C. Fangmeier, F. Golf, R. Gonzalez Suarez, R. Kamalieddin, I. Kravchenko, J. Monroy, J.E. Siado, G.R. Snow, B. Stieger

State University of New York at Buffalo, Buffalo, USA
A. Godshalk, C. Harrington, I. Iashvili, A. Kharchilava, D. Nguyen, A. Parker, S. Rappoccio, B. Roozbahani

Northeastern University, Boston, USA
G. Alverson, E. Barberis, C. Freer, A. Hortiangtham, D.M. Morse, T. Orimoto, R. Teixeira De Lima, T. Wamorkar, B. Wang, A. Wisecarver, D. Wood

Northwestern University, Evanston, USA
S. Bhattacharya, O. Charaf, K.A. Hahn, N. Mucia, N. Odell, M.H. Schmitt, K. Sung, M. Trovato, M. Velasco

University of Notre Dame, Notre Dame, USA
R. Bucci, N. Dev, M. Hildreth, K. Hurtado Anampa, C. Jessop, D.J. Karmgard, N. Kellams, K. Lannon, W. Li, N. Loukas, N. Marinelli, F. Meng, C. Mueller, Y. Musienko[34], M. Planer, A. Reinsvold, R. Ruchti, P. Siddireddy, G. Smith, S. Taroni, M. Wayne, A. Wightman, M. Wolf, A. Woodard

The Ohio State University, Columbus, USA
J. Alimena, L. Antonelli, B. Bylsma, L.S. Durkin, S. Flowers, B. Francis, A. Hart, C. Hill, W. Ji, T.Y. Ling, W. Luo, B.L. Winer, H.W. Wulsin

Princeton University, Princeton, USA
S. Cooperstein, P. Elmer, J. Hardenbrook, S. Higginbotham, A. Kalogeropoulos, D. Lange, M.T. Lucchini, J. Luo, D. Marlow, K. Mei, I. Ojalvo, J. Olsen, C. Palmer, P. Piroué, J. Salfeld-Nebgen, D. Stickland, C. Tully

University of Puerto Rico, Mayaguez, USA
S. Malik, S. Norberg

Purdue University, West Lafayette, USA
A. Barker, V.E. Barnes, S. Das, L. Gutay, M. Jones, A.W. Jung, A. Khatiwada, B. Mahakud, D.H. Miller, N. Neumeister, C.C. Peng, H. Qiu, J.F. Schulte, J. Sun, F. Wang, R. Xiao, W. Xie

Purdue University Northwest, Hammond, USA
T. Cheng, J. Dolen, N. Parashar

Rice University, Houston, USA
Z. Chen, K.M. Ecklund, S. Freed, F.J.M. Geurts, M. Kilpatrick, W. Li, B. Michlin, B.P. Padley, J. Roberts, J. Rorie, W. Shi, Z. Tu, J. Zabel, A. Zhang

University of Rochester, Rochester, USA
A. Bodek, P. de Barbaro, R. Demina, Y.t. Duh, J.L. Dulemba, C. Fallon, T. Ferbel, M. Galanti, A. Garcia-Bellido, J. Han, O. Hindrichs, A. Khukhunaishvili, K.H. Lo, P. Tan, R. Taus, M. Verzetti

Rutgers, The State University of New Jersey, Piscataway, USA
A. Agapitos, J.P. Chou, Y. Gershtein, T.A. Gómez Espinosa, E. Halkiadakis, M. Heindl, E. Hughes, S. Kaplan, R. Kunnawalkam Elayavalli, S. Kyriacou, A. Lath, R. Montalvo, K. Nash, M. Osherson, H. Saka, S. Salur, S. Schnetzer, D. Sheffield, S. Somalwar, R. Stone, S. Thomas, P. Thomassen, M. Walker

University of Tennessee, Knoxville, USA
A.G. Delannoy, J. Heideman, G. Riley, S. Spanier, K. Thapa

Texas A&M University, College Station, USA
O. Bouhali[72], A. Celik, M. Dalchenko, M. De Mattia, A. Delgado, S. Dildick, R. Eusebi, J. Gilmore, T. Huang, T. Kamon[73], S. Luo, R. Mueller, R. Patel, A. Perloff, L. Perniè, D. Rathjens, A. Safonov

Texas Tech University, Lubbock, USA
N. Akchurin, J. Damgov, F. De Guio, P.R. Dudero, S. Kunori, K. Lamichhane, S.W. Lee, T. Mengke, S. Muthumuni, T. Peltola, S. Undleeb, I. Volobouev, Z. Wang

Vanderbilt University, Nashville, USA
S. Greene, A. Gurrola, R. Janjam, W. Johns, C. Maguire, A. Melo, H. Ni, K. Padeken, J.D. Ruiz Alvarez, P. Sheldon, S. Tuo, J. Velkovska, M. Verweij, Q. Xu

University of Virginia, Charlottesville, USA
M.W. Arenton, P. Barria, B. Cox, R. Hirosky, M. Joyce, A. Ledovskoy, H. Li, C. Neu, T. Sinthuprasith, Y. Wang, E. Wolfe, F. Xia

Wayne State University, Detroit, USA
R. Harr, P.E. Karchin, N. Poudyal, J. Sturdy, P. Thapa, S. Zaleski

University of Wisconsin - Madison, Madison, WI, USA
M. Brodski, J. Buchanan, C. Caillol, D. Carlsmith, S. Dasu, L. Dodd, B. Gomber, M. Grothe, M. Herndon, A. Hervé, U. Hussain, P. Klabbers, A. Lanaro, A. Levine, K. Long, R. Loveless, T. Ruggles, A. Savin, N. Smith, W.H. Smith, N. Woods

†: Deceased
1: Also at Vienna University of Technology, Vienna, Austria
2: Also at IRFU, CEA, Université Paris-Saclay, Gif-sur-Yvette, France
3: Also at Universidade Estadual de Campinas, Campinas, Brazil
4: Also at Federal University of Rio Grande do Sul, Porto Alegre, Brazil
5: Also at Université Libre de Bruxelles, Bruxelles, Belgium
6: Also at University of Chinese Academy of Sciences, Beijing, China
7: Also at Institute for Theoretical and Experimental Physics, Moscow, Russia
8: Also at Joint Institute for Nuclear Research, Dubna, Russia
9: Now at Cairo University, Cairo, Egypt
10: Now at Helwan University, Cairo, Egypt
11: Now at Fayoum University, El-Fayoum, Egypt
12: Also at Department of Physics, King Abdulaziz University, Jeddah, Saudi Arabia
13: Also at Université de Haute Alsace, Mulhouse, France
14: Also at Skobeltsyn Institute of Nuclear Physics, Lomonosov Moscow State University, Moscow, Russia
15: Also at CERN, European Organization for Nuclear Research, Geneva, Switzerland
16: Also at RWTH Aachen University, III. Physikalisches Institut A, Aachen, Germany
17: Also at University of Hamburg, Hamburg, Germany
18: Also at Brandenburg University of Technology, Cottbus, Germany
19: Also at MTA-ELTE Lendület CMS Particle and Nuclear Physics Group, Eötvös Loránd University, Budapest, Hungary
20: Also at Institute of Nuclear Research ATOMKI, Debrecen, Hungary
21: Also at Institute of Physics, University of Debrecen, Debrecen, Hungary
22: Also at Indian Institute of Technology Bhubaneswar, Bhubaneswar, India

23: Also at Institute of Physics, Bhubaneswar, India
24: Also at Shoolini University, Solan, India
25: Also at University of Visva-Bharati, Santiniketan, India
26: Also at Isfahan University of Technology, Isfahan, Iran
27: Also at Plasma Physics Research Center, Science and Research Branch, Islamic Azad University, Tehran, Iran
28: Also at Università degli Studi di Siena, Siena, Italy
29: Also at Kyunghee University, Seoul, Korea
30: Also at International Islamic University of Malaysia, Kuala Lumpur, Malaysia
31: Also at Malaysian Nuclear Agency, MOSTI, Kajang, Malaysia
32: Also at Consejo Nacional de Ciencia y Tecnología, Mexico city, Mexico
33: Also at Warsaw University of Technology, Institute of Electronic Systems, Warsaw, Poland
34: Also at Institute for Nuclear Research, Moscow, Russia
35: Now at National Research Nuclear University 'Moscow Engineering Physics Institute' (MEPhI), Moscow, Russia
36: Also at St. Petersburg State Polytechnical University, St. Petersburg, Russia
37: Also at University of Florida, Gainesville, USA
38: Also at P.N. Lebedev Physical Institute, Moscow, Russia
39: Also at California Institute of Technology, Pasadena, USA
40: Also at Budker Institute of Nuclear Physics, Novosibirsk, Russia
41: Also at Faculty of Physics, University of Belgrade, Belgrade, Serbia
42: Also at INFN Sezione di Pavia [a], Università di Pavia [b], Pavia, Italy
43: Also at University of Belgrade, Faculty of Physics and Vinca Institute of Nuclear Sciences, Belgrade, Serbia
44: Also at Scuola Normale e Sezione dell'INFN, Pisa, Italy
45: Also at National and Kapodistrian University of Athens, Athens, Greece
46: Also at Riga Technical University, Riga, Latvia
47: Also at Universität Zürich, Zurich, Switzerland
48: Also at Stefan Meyer Institute for Subatomic Physics (SMI), Vienna, Austria
49: Also at Istanbul Aydin University, Istanbul, Turkey
50: Also at Mersin University, Mersin, Turkey
51: Also at Piri Reis University, Istanbul, Turkey
52: Also at Gaziosmanpasa University, Tokat, Turkey
53: Also at Adiyaman University, Adiyaman, Turkey
54: Also at Ozyegin University, Istanbul, Turkey
55: Also at Izmir Institute of Technology, Izmir, Turkey
56: Also at Marmara University, Istanbul, Turkey
57: Also at Kafkas University, Kars, Turkey
58: Also at Istanbul University, Faculty of Science, Istanbul, Turkey
59: Also at Istanbul Bilgi University, Istanbul, Turkey
60: Also at Hacettepe University, Ankara, Turkey
61: Also at Rutherford Appleton Laboratory, Didcot, United Kingdom
62: Also at School of Physics and Astronomy, University of Southampton, Southampton, United Kingdom
63: Also at Monash University, Faculty of Science, Clayton, Australia
64: Also at Bethel University, St. Paul, USA
65: Also at Karamanoğlu Mehmetbey University, Karaman, Turkey
66: Also at Utah Valley University, Orem, USA
67: Also at Purdue University, West Lafayette, USA

68: Also at Beykent University, Istanbul, Turkey
69: Also at Bingol University, Bingol, Turkey
70: Also at Sinop University, Sinop, Turkey
71: Also at Mimar Sinan University, Istanbul, Istanbul, Turkey
72: Also at Texas A&M University at Qatar, Doha, Qatar
73: Also at Kyungpook National University, Daegu, Korea